Journal of Physical and Chemical Reference Data ARTICLE pubs.aip.org/aip/jpr

Cross Sections for Electron Collisions with the CO_2 Molecule and CO_2^+ Molecular Ion

Cite as: J. Phys. Chem. Ref. Data 53, 033102 (2024); doi: 10.1063/5.0215796
Submitted: 26 April 2024 • Accepted: 14 June 2024 •
Published Online: 20 August 2024

Mi-Young Song,[1,a)] Hyuck Cho,[2] Grzegorz P. Karwasz,[3] Viatcheslav Kokoouline,[4] and Jonathan Tennyson[5]

AFFILIATIONS

[1] Institute of Plasma Technology, Korea Institute of Fusion Energy (KFE), 37, Dongjangsan-ro, Gunsan, Jeollabuk-do 54004, South Korea
[2] Department of Physics, Chungnam National University, Daejeon 34134, South Korea
[3] Institute of Physics, Astronomy and Applied Informatics, Nicolaus Copernicus University, Grudziadzka 5, 87-100 Toruń, Poland
[4] Department of Physics, University of Central Florida, Orlando, Florida 32816, USA
[5] Department of Physics and Astronomy, University College London, Gower Street, London WC1E 6BT, United Kingdom

[a)] **Author to whom correspondence should be addressed:** mysong@kfe.re.kr

ABSTRACT

Electron collision cross section data are complied from the literature for electron collisions with the carbon dioxide molecule, CO_2 and the CO_2^+ ion. Cross sections are collected and reviewed for total scattering, elastic scattering, momentum transfer, rotational excitation, vibrational excitation, electronic excitation, dissociative processes and ionization. The literature has been surveyed up to the end 2023. For each of these processes, the recommended values of the cross sections are presented with an estimated uncertainty.

Published by AIP Publishing on behalf of the National Institute of Standards and Technology. https://doi.org/10.1063/5.0215796

CONTENTS

List of Tables

List of Figures

1. Introduction

Carbon dioxide, CO_2, is considered to be the main driver of global warming. This is only partially true, as other gases, like methane (CH_4) or nitrous oxide (N_2O) have greater warming potential and similarly long permanence times in troposphere (stratosphere). However, huge amount of the carbon dioxide added to the atmosphere from the beginning of the industrial era (raising its concentration from 280 to 420 ppm currently) makes urgent the search for efficient processes of chemical/physical/geological sequestering or valorisation of CO_2.

Knowledge of CO_2 molecular properties and of the products of its dissociation, ionization, excitation is crucial for developing such technologies. Numerous works[1,2] are under way to project methods of CO_2 sequestration via plasma technologies. A particular aspect of the removal is the subject of plasma assisted valorisation of CO_2 which aims not just to remove CO_2 from the atmosphere but to transform it into a chemically useful species such as hydrocarbons, using a suitable mixture of plasma processing and catalysis. Models of plasma-assisted CO_2 valorisation to usable produce products such as hydrocarbons or methanol require significant amount of data on electron collisions with CO_2.[1,3,4] The need for data has led to

Published by AIP Publishing on behalf of the National Institute of Standards and Technology.

recent studies of electron collisions with vibrationally excited states of CO_2.[5,6]

For more than 50 years the technology of cutting using powerful CO_2 lasers (kW of continuous power focused down to less a millimeter diameter) has been practiced. This technology developed rapidly in 1960s, presumably at least in part for military purposes. However, the laser wavelength region (10.6 μm) made such an application (until recently) impractical. The operation of the CO_2 lasers requires a well determined admixture of He and N_2 (65% and 32% respectively). The laser emission comes from rotational sublevels of vibrational transitions of the CO_2 molecule,[7] but the particularity of electron interactions with carbon dioxide gives rise to a very strong resonance at an electron collision energy of around 3.7 eV which enhances these transitions. Furthermore, vibrational excitation also results from collisions with N_2 molecules,[8,9] which shows a similar resonance.[10] As we discuss in this paper, the knowledge of these excitations was until recently quite fragmentary. The Martian atmosphere is predominantly of CO_2. From the perspective of Mars exploration, it has been suggested that the CO_2 in the atmosphere could be used as a source of oxygen, and together with N_2 – as a source of fertilizers.[11]

Due to its importance, numerous works reviewed,[12,13] tabulated,[14] compared,[15] derived from diffusion coefficients[16–18] or gave "complete" sets[19] of electron-scattering cross sections for the CO_2 molecule. However, these cross sections are still far from being exhaustive; only fragmentary data are available for the CO_2^+ ion.

The present review, mainly of experimental work but with the use of theory to evaluate and, if needed, substitute experiments, gives recommended cross sections. For CO_2, we consider total, elastic, momentum transfer, vibrational and rotational excitations, dissociative electron attachment, electronic levels excitation, ionization, dissociation into neutral fragments; while for the CO_2^+ ion dissociative recombination cross sections are also considered. The present work is continuation of previous compilations, on carbon-containing molecules (CH_4, see Ref. 20 and C_2H_2, see Ref. 21) and on molecules of the atmospheric importance (N_2, see Ref. 10, NO, N_2O and NO_2, see Ref. 22), and water.[23]

2. CO_2 Molecule

2.1. Total scattering cross section

Measurements of total cross sections (TCS) are relatively easy as compared, for example, to the integral elastic or vibrational excitation cross sections, even if they require using precise methodologies. In the attenuation method the current of electrons is monitored vs the density of the gas in the scattering cell, see for example Ref. 20 for details of experiments. Generally, the measurements of TCS do not require normalization or extrapolation procedures like those of integral elastic cross sections.

Numerous laboratories studied TCS in CO_2, using several, alternative methods. Hoffman *et al.*[24] and Kwan *et al.*[25] used an apparatus with a weak longitudinal magnetic field, designed for electron and positron scattering, in the energy range 2–50 eV and 100–500 eV, respectively. A similar apparatus (but with a short scattering cell) was used by Sueoka and Mori[26] in the 1–400 eV energy range; those data have been later refined by Kimura *et al.*[27] Szmytkowski *et al.*[28] reported TCS from two laboratories: Gdańsk, using an electrostatic energy-selector in the range 0.5–80 eV, and Trento, using a Ramsauer method (i.e., a perpendicular magnetic field, without an electrostatic retarding analyser) in the range 75–3000 eV. Alternatively, in the high energy range (400–5000 eV) García and Manero[29] used an electrostatic energy selector with a retarding-field analyzer, i.e., discriminating electrons scattered inelastically in the forward direction.

The agreement between TCS obtained by beam techniques, see Fig. 1, from different laboratories is good, keeping in mind the intrinsic sources of uncertainties (dynamic processes of the outflow of gas from the scattering cells, temperature instabilities, non-equilibrium conditions of the pressure measurements, forward-scattering uncertainties when using the magnetic guiding field etc.)

A recent experiment, with 80 meV energy resolution, by Lozano *et al.*,[33] used a short (40 mm length) scattering cell and a strong (up to 1 kG) confining magnetic field:[34] the data need corrections for forward scattering. TCS by Lozano *et al.*[33] coincide within their declared experimental uncertainty (5%) with previously recommended values,[35] apart from a few points near the low energy limit which are somewhat lower than other experiments. Lozano *et al.*[33] observed also a tiny, resonance-like maximum at 8.5 eV (see Fig. 1 in their paper), i.e., at the energy at which the peak of the dissociative attachment is seen (see later in this paper); this structure was not reported by other experimental studies.

The only data visibly outside the ±5% band in the Fig. 1, are those by Sueoka and Mori[26] (which was obtained using positron-scattering apparatus): Sueoka and Mori[26] adopted the length of the scattering cell on the basis of normalization to other laboratories, which affected both the energy scale (in the time-of-flight experiment) and absolute values. Figure 1 does not present the early data by Brüche[36] between 1 and 50 eV, by Ramsauer[37] around 1 eV, and

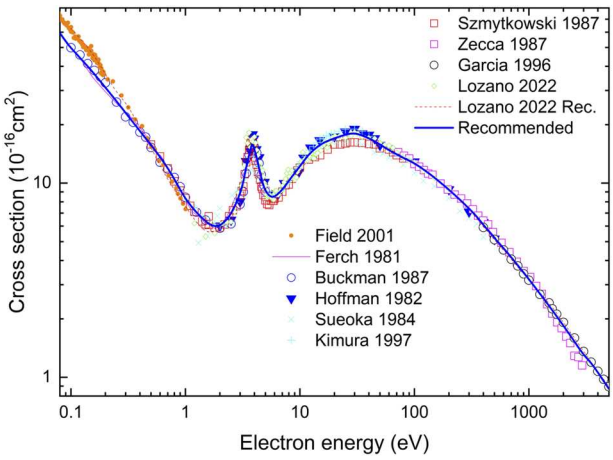

FIG. 1. Comparison of experimental TCS for electron scattering on CO_2: red small circles, very low energy TCS by Field *et al.*;[30] thin magenta line, Ref. 31; open blue circles, Ref. 32; "Hoffman," inverted blue triangle denotes Detroit data;[24,25] small cyan symbols are from Sueoka's lab;[26,27] red open squares are from Gdańsk lab and magenta squares from Trento lab in the paper by Szmytkowski *et al.*;[28] open black circles - high energy TCS by García and Manero;[29] small green diamonds - recent low energy data from the same lab[33] and red dotted line are TCS recommended by them;[33] the thick blue line is our recommended TCS.

Published by AIP Publishing on behalf of the National Institute of Standards and Technology.

by Ramsauer and Kollath[38] at 0.18–2 eV, even though the interesting features of CO_2 total cross section, i.e., the $^2\Pi_u$ shape-resonance state, and the rise of the TCS in the limit of zero energy were first identified by those authors.

In the very low energy limit, the measurements with a resolution of 1.5 meV by Field *et al.*,[30] who used a synchrotron-radiation electron source, are somewhat higher that the time-of-flight experiments by Ferch *et al.*[31] and Buckman *et al.*[32] This discrepancy remains within the combined experimental uncertainties (8% being the statistical spread in the data of Field *et al.*[30])

The most recent experiment by Kitajima *et al.*,[39] used the same technique as Field *et al.*,[30] but performed measurements with good statistics (the overall statistical and systematic uncertainty of about 2%). The measurements[39] agree with other experiments, except in the region of the $^2\Pi_u$ resonance, where their maximum of the TCS is higher than other data, and slightly shifted to lower energies, see the discussion below.

In the maximum of the $^2\Pi_u$ resonance, the measured TCS depends on the energy resolution of particular apparati (and on the grid of energies chosen): Hoffman *et al.*[24] reported 17.8×10^{-16} cm^2 at 3.85 eV, Szmytkowski *et al.*[28] 16.7×10^{-16} cm^2 at 3.8 eV, Buckman *et al.*[32] 15.4×10^{-16} cm^2 and Lozano *et al.*[33] 16.8×10^{-16} cm^2 at the same energy. (Note a shifted position of the maximum in the latter data, see Fig. 2.) The maximum of recommended TCS, obtained by averaging measurements performed with detailed energy grid[28,31,32] amounts to 15.8×10^{-16} cm^2 at 3.8 eV. The recent TCS extending to very low energies by Kitajima *et al.*[39] are not included in this averaging, for reasons explained below.

At about 20 eV Kimura *et al.*[27] claimed higher values than those of Szmytkowski *et al.*,[28] in agreement with measurements of Hoffman *et al.*[24] Therefore, the recommended values in the intermediate energy range were obtained by averaging over these three data sets: the newest measurements by Lozano *et al.*[33] confirm our recommended TCS.

In the high energy limit presently recommended TCS are based on the data by García and Manero:[29] as already mentioned the apparatus by Zecca and collaborators[28] lacked a retarding-field analyzer. We use Bethe-Born fit Eq. (1) as an auxiliary mean to evaluate the high energy data, similarly as for the gases reviewed before,[20,21] see Fig. 2.

The Born-Bethe fit reduced to two terms reads

$$\sigma(E) = \frac{A}{E} + B\frac{\log E}{E} \qquad (1)$$

where the energy is expressed in Rydbergs, $R = 13.6$ eV, and the cross sections is expressed in atomic units $a_0^2 = 0.28 \times 10^{-16}$ cm^2. This fit allows identification of possible systematic errors in the high energy limit and extrapolation of the TCS up to a few tens of keV, see Fig. 2. As seen from this figure, the TCS in the high energy range can be well fitted by a straight-line with $A = -100 \pm 10$ and $B = 510 \pm 25$ [in the units of Eq. (1)]. Figure 2 gives a comparison between CO and CO_2, showing that the high-energy parameter B scales, approximately, as the total number of electrons in the target (for CO the parameters of the fit are $A = -67 \pm 10$ and $B = 370 \pm 10$).

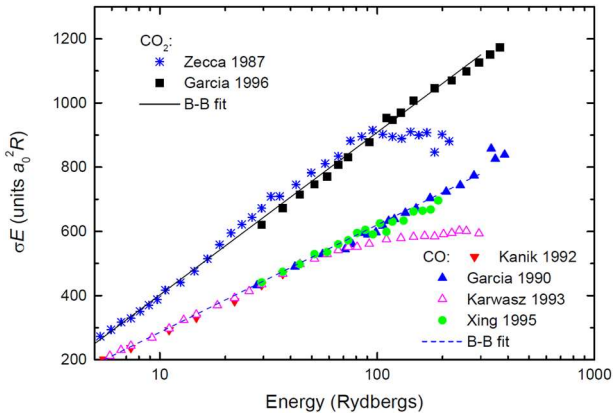

FIG. 2. Comparison of experimental TCS for electron scattering on CO_2 and CO in the high-energy range, Eq. (1). "Zecca" denotes high-energy data from the Trento laboratory presented in the paper by Szmytkowski *et al.*;[28] "Garcia" is Ref. 40 for CO and Ref. 29 for CO_2; other data for CO are Kanik *et al.*,[41] Karwasz *et al.*,[42] Xing *et al.*[43]

TABLE 1. Recommended (in 10^{-16} cm^2) TCS for electron scattering on CO_2. The values are based on the review by Karwasz *et al.*[35] Uncertainties are ±5% over the whole energy range, apart from the resonance region and energies below 0.5 eV, see text. A finer grid is given in the supplementary material

Electron energy (eV)	TCS (10^{-16} cm^2)	Electron energy (eV)	TCS (10^{-16} cm^2)
0.10	49.7	12	14.2
0.12	44.3	15	15.8
0.15	38.1	17	16.4
0.17	34.9	20	17.0
0.20	31.1	25	17.8
0.25	26.4	30	18.0
0.30	23.0	35	17.6
0.35	20.5	40	17.0
0.40	18.6	45	16.4
0.50	15.7	50	15.8
0.60	13.6	60	14.8
0.70	11.9	70	14.1
0.80	10.5	80	13.5
0.90	9.25	90	13.1
1.0	8.29	100	12.6
1.2	7.22	120	11.8
1.5	6.32	150	10.6
1.7	6.02	170	10.0
2.0	5.94	200	9.24
2.5	6.81	250	8.20
3.0	8.77	300	7.39
3.5	13.3	350	6.73
4.0	14.9	400	6.08
4.5	11.3	450	5.62
5.0	9.06	500	5.23
6.0	8.44	600	4.63
7.0	9.21	700	4.16
8.0	10.3	800	3.78
9.0	11.3	900	3.47
10	12.2	1000	3.20

Published by AIP Publishing on behalf of the National Institute of Standards and Technology.

The uncertainty on the present recommended data is ±5%, apart from the region below 0.5 eV and in the $^2\Pi_u$ resonance peak that we estimate it as ±10% (Table 1).

The CO_2 molecule is non-polar, but in its vibrationally excited state in the bending modes (see later for details) a transition dipole moment appears. As the threshold for the bending (01^10) mode is low (160 meV), already in moderate temperatures a significant fraction (about 22% at 520 K) of the CO_2 molecule is in the vibrationally excited state. Two laboratories measured TCS at elevated temperatures. Buckman *et al.*[32] noticed a rise by about 10% of the TCS below 2 eV for scattering at 573 K. Ferch *et al.*[44] made a deconvolution of the TCS measured at 520 K and derived the TCS for scattering on the vibrationally bent molecule, see Fig. 3. Taking into account the population of the vibrational sub-levels, the main contribution (73%) to the TCS for the vibrationally excited molecule comes from the (011^10) mode with small admixtures (13% and 8%) of the (02^20) and (02^00) modes, respectively (see Ref. 44 for details).

The TCS for vibrationally excited CO_2 molecule is higher than for the ground state, particularly at low energies. Further, the position of the shape resonance peak moves to lower energy by some 0.3 eV, see Fig. 3.

As already mentioned, the most recent measurements (at 298 K) with the photo-electron source and 2 meV energy resolution by Kitajima *et al.*[39] differ in amplitude and the energy position of the $^2\Pi_u$ resonance, see Fig. 3. Further, they observed a vibrational structure in this resonance, similar to the structure in the $^2\Pi_u$ resonance in N_2.[45] Observation of this structure, which is not seen in other experiments, can be explained by the extremely high energy resolution,[39] but the origin of the shift is unclear. We can only hypothesize that earlier measurements, usually using diffusion pumps, may have been performed at lower that 298 K temperature of the gas in the scattering cell. Therefore, in the region of the $^2\Pi_u$ resonance we recommend the data by Kitajima *et al.*,[39] see Table 2.

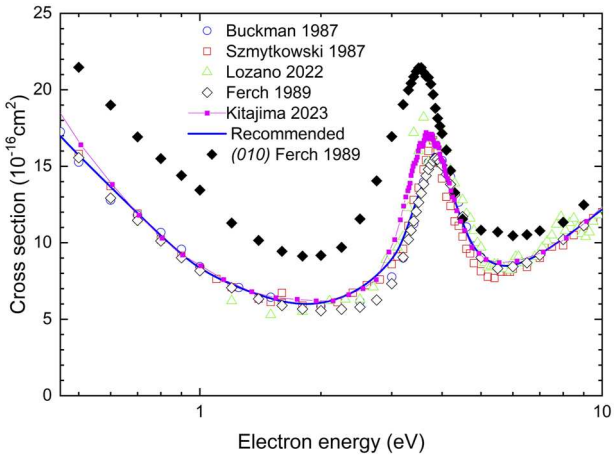

FIG. 3. TCS for CO_2 molecule in its ground (000) vibrational state, open symbols: blue circles Ref. 32, red squares Ref. 28, green triangles Ref. 33, black diamonds Ref. 44, magenta small squares with line Ref. 39, blue line - present recommended values; closed symbols, TCS in the excited vibrational bent state, Ref. 44, see text for details.

TABLE 2. TCS for electron scattering on CO_2 below 20 eV. The values are those from high resolutions measurements at 298 K by Kitajima *et al.*[39] Uncertainties are within ±5% in the whole energy range

Electron energy (eV)	TCS (10^{-16} cm^2)	Electron energy (eV)	TCS (10^{-16} cm^2)
20.144	17.2	3.470	15.6
18.144	16.9	3.450	15.4
16.144	16.6	3.430	15.2
15.144	16.2	3.410	15.2
14.144	15.6	3.390	15.0
13.144	15.2	3.370	14.7
12.144	14.5	3.350	14.4
11.144	13.4	3.330	13.9
10.144	12.5	3.310	13.6
9.144	11.4	3.290	13.4
8.144	10.3	3.250	13.0
7.144	9.4	3.210	12.4
6.144	8.8	3.150	11.5
5.544	8.7	3.050	10.2
5.144	8.9	2.950	9.4
4.944	9.3	2.744	7.6
4.750	9.7	2.544	7.0
4.550	10.8	2.344	6.6
4.450	11.4	2.144	6.2
4.350	12.1	1.946	6.2
4.290	12.8	1.746	6.3
4.250	13.0	1.546	6.4
4.210	13.4	1.346	6.8
4.170	13.9	1.146	7.6
4.130	14.2	1.006	8.5
4.090	14.4	0.906	9.2
4.070	14.7	0.806	10.3
4.050	15.0	0.706	11.8
4.030	15.3	0.606	13.8
4.010	15.3	0.506	16.4
3.990	15.4	0.406	20.3
3.970	15.5	0.366	22.6
3.950	15.8	0.324	25.8
3.930	16.2	0.304	27.1
3.910	16.4	0.284	27.7
3.890	16.5	0.264	29.6
3.870	16.4	0.244	32.5
3.850	16.3	0.224	34.5
3.830	16.4	0.204	37.5
3.810	16.7	0.183	42.1
3.790	17.0	0.163	45.2
3.770	17.1	0.143	49.3
3.750	17.0	0.123	54.5
3.730	16.8	0.103	61.0
3.710	16.8	0.093	65.4
3.690	16.8	0.083	68.5
3.670	17.1	0.073	71.5
3.650	17.2	0.063	78.2
3.630	17.0	0.053	85.2
3.610	16.7	0.043	93.3
3.590	16.4	0.033	101.9

Published by AIP Publishing on behalf of the National Institute of Standards and Technology.

TABLE 2. (*Continued*)

Electron energy (eV)	TCS (10^{-16} cm^2)	Electron energy (eV)	TCS (10^{-16} cm^2)
3.570	16.3	0.023	109.9
3.550	16.4	0.019	115
3.530	16.5	0.017	119
3.510	16.3	0.013	119
3.490	16.0	0.009	124

Furthermore, Johnstone *et al.*[46] studied elastic scattering from the (010) vibrationally excited molecule (by heating the gas to about 500 K). At the collision energy of 3.8 eV (i.e., at the $^2\Pi_u$ resonance) they observed not only a higher differential cross section (DCS) (by a factor of 10 at 60°, primarily), but an essential change in the shape of this cross section, which becomes forward-peaked for the excited molecule (we recall - with the vibration-induced transition dipole moment) as compared to the ground-state molecule, which exhibits a rather uniform in angle DCS for elastic scattering at this energy, see Fig. 3 in Ref. 46. In turn, forward-peaked DCS may lead to underestimation of TCS, especially in measurements with a moderate angular resolution.[24,28,33]

The rise of the TCS in the very low range was attributed, shortly after the experimental observation,[31] to a virtual state.[47–49] Resonant phenomena have been experimentally observed in vibrational excitation[50] and in recent TCS measurements at very low energies.[39] Semi-empirical analysis using modified effective range theory[51] gave a scattering length of $6.6a_0$, i.e., the TCS (or better: the integral elastic cross section) of about 150×10^{-16} cm^2 at zero energy, see also Ref. 52 for a more recent comparison.

Summarizing, for the sake of modeling plasma and atmospheric processes the consistency of listed TCSs is to be considered satisfactory. However, even if the measurements of TCS seemed to be "easy," still existing discrepancies trigger some questions, especially in the presence of resonance phenomena in electron scattering on CO_2. The authors recommend further contributions both from experiments and the theory.

2.2. Elastic scattering cross section

There have been many experimental and theoretical studies on the elastic scattering processes of electrons with carbon dioxide gases to measure or calculate their differential and integral cross sections. Among them, we considered only those more or less relevant to our interest of energy regions. A rather old measurement made by Shyn *et al.*[53] who measured the DCS for electron energies from 3.0 to 90 eV and for scattering angles from 12° to 156°, but their measurements are relative. For the absolute measurement of the cross sections, we considered the following results: Register *et al.*,[54] for the energy range 4–50 eV and for the scattering angles from 15° to 140°, Kochem *et al.*[55] for only two threshold energies of 0.155 and 1.05 eV and 15°–100° angles, Kanik *et al.*[56] for 20–100 eV energy range and 20°–120° angular range, Tanaka *et al.*[57] for 1.5–100 eV energy range and 15°–130° angular range, Gibson *et al.*[58] for the energy range of 1.0–50 eV and the angular range from 10° to 130°, and Iga *et al.*[59] in the rather high energy region of 100–400 eV for 10°–120° angles. In most of these experimental measurements electron spectrometers were used with the relative-flow technique to put the measurements on an absolute scale as described, for example, in Tanaka *et al.*[57] Theoretically, Takekawa and Itikawa[60] calculated the cross section for 3–60 eV energy region, based on an *ab initio* electrostatic potential taken with the approximate effects of electron exchange and target polarization. Iga *et al.*[59] not only made experimental studies but also calculated the cross sections for the energy range 30–500 eV, using a complex optical potential consisting of static, exchange, correlation–polarization plus absorption contributions. Rescigno *et al.*[61] used the complex Kohn variational method from 0.25 to 10 eV region and Gianturco and Stoecklin[62] revisited the CO_2 scattering behavior for the elastic channels using exact static exchange interaction and a global density functional modeling of correlation-polarization. Previous efforts compiling these experimental and theoretical results to derive recommended cross sections were conducted by Shirai *et al.*,[14] Itikawa,[13] and very recently Lozano *et al.*[33] Shirai *et al.* evaluated cross section data in the energy range above 1 eV and gave a short review of the cross section measurements. Itikawa presented a rather extensive review on the various processes of electron scattering with CO_2; while Lozano *et al.* updated the recommended TCS (for 0.1–5000 eV) based on the recommendation of Itikawa[13] (for 0.1–1000 eV), their own new measurement (for 1.2–200 eV), and calculation using independent atom model with the screening corrected additive rule including interference (IAM-SCAR+I) effects. From this updated TCS, Lozano *et al.* obtained a self-consistent integral cross sections (ICS) for the elastic and inelastic processes. Among the previous DCS measurements mentioned above, Register *et al.*,[54] Tanaka *et al.*,[57] and Gibson *et al.*[58] generally agree with each other reasonably well in the energy range of their measurement. However, at 5 eV the disagreement between Tanaka *et al.* and Gibson *et al.* is clearly significant. Near the scattering angle of 50° Tanaka *et al.* show a clear peak while Gibson *et al.* show only a slight indication of the peak. This same kind of disagreement appears also at 3.8 eV where shape resonance of $^2\Pi_u$ appears and the theoretical results rather supports Tanaka *et al.* than Gibson *et al.* We suggest that this disagreement might be due to the differences in the resolutions of the electron spectrometer used in these two groups: the spectrometer resolutions of Tanaka *et al.* and Gibson *et al.* are 33 and 40–60 meV, respectively. Obviously, with lower resolution peaks can be flattened which could be the case in the result of Gibson *et al.* To obtain our recommended DCS we averaged Register *et al.*,[54] Tanaka *et al.*,[57] and Gibson *et al.*[58] at low to medium energies, except at 5 eV where we recommend Tanaka *et al.* Recommended DCSs are given in the Fig. 4 and Table 3 with the corresponding uncertainties.

For the recommended elastic integral cross section (ICS), Itikawa[13] used the results by Buckman *et al.*[63] for 1–60 eV region and Shirai *et al.*[14] for 100-1000 eV region. Itikawa estimated uncertainties to be less than 30% for 1–60 eV and 18% for energies higher than 100 eV. Shirai *et al.* evaluated ICS up to 1000 eV based on Iga *et al.*[59,64] Recently, Lozano *et al.*[33] extended the recommendation of Itikawa from 1 to 0.1 eV in the low-energy region and from 1000 to 5000 eV in the high-energy region, respectively, using the IAM-SCAR+I. However, as the authors themselves mentioned, IAM-SCAR+I theory is generally valid for the energies above 20 eV, therefore the ICS recommendation by Lozano *et al.* in the energy region 0.1–1 eV cannot be trusted. Nevertheless, Lozano *et al.*'s

Published by AIP Publishing on behalf of the National Institute of Standards and Technology.

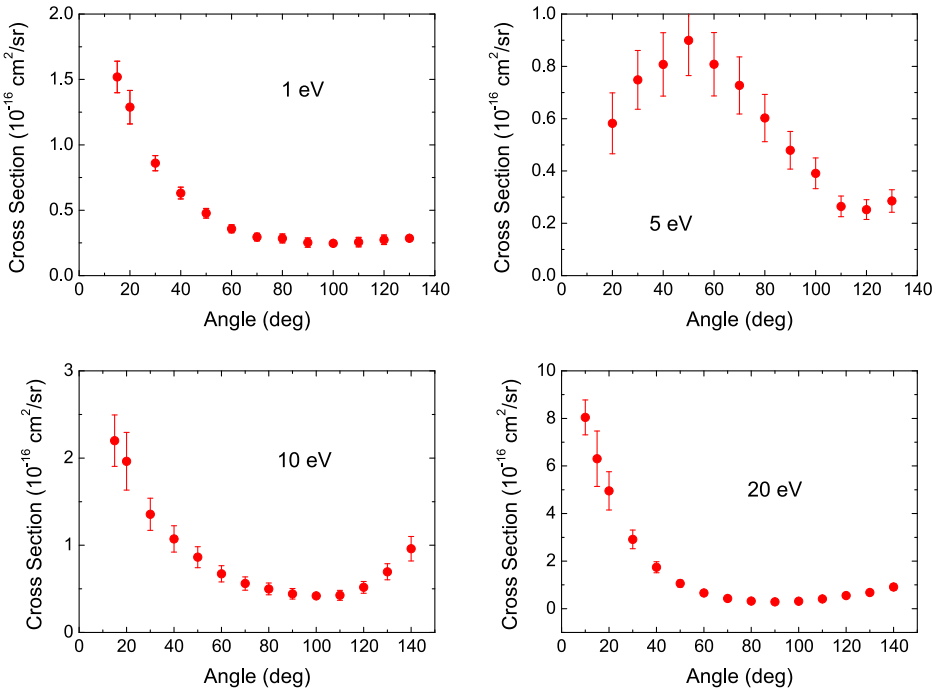

FIG. 4. Recommended elastic DCS of CO_2 for the represented incident electron energies. Uncertainties are given by the vertical bars (10^{-16} cm^2/sr).

recommendations are the same as the present recommendations, except for the energy range 3–5 eV and at 1 eV. Within 3–5 eV, Lozano *et al.* considered the resonant contribution to the TCS as electron attachment instead of elastic scattering. For the high energy side from 1000 to 5000 eV, the theory should be reasonably good and also at 1000 eV Lozano *et al.* agree with Itikawa.[13] Therefore, Itikawa[13] in 1–1000 eV with Lozano *et al.*[33] in 1000–5000 eV are suggested as our ICS recommendation. Recommended ICSs are given in the Fig. 5 and Table 4.

2.3. Momentum transfer cross section

The elastic momentum transfer cross section (MTCS) of CO_2 have been measured either by electron-molecule crossed beam experiments or by swarm methods. The experimental groups which

TABLE 3. Recommended elastic DCSs of CO_2 (10^{-16} cm^2 sr^{-1}). δ means uncertainties

	1.0 eV		2.0 eV		5.0 eV		10 eV		20 eV		50 eV		100 eV		400 eV	
Angle (°)	DCS	δ	DCS	δ	DCS	δ	DCS	δ	DCS	δ	DCS	δ	DCS	δ	DCS	δ
10							1.927	0.160	8.043	0.732	10.57	0.983			7.19	0.74
15	1.519	0.120	1.244	0.547			2.199	0.295	6.306	1.166	6.350	0.950	6.797	0.923	2.377	0.244
20	1.288	0.128	0.799	0.115	0.5824	0.1165	1.963	0.331	4.951	0.805	4.435	0.556	3.484	0.481	1.040	0.107
30	0.860	0.058	0.506	0.062	0.7486	0.1123	1.355	0.184	2.914	0.392	1.761	0.219	0.941	0.126	0.455	0.046
40	0.631	0.045	0.336	0.043	0.8076	0.1211	1.073	0.151	1.742	0.232	0.796	0.096	0.366	0.049	0.215	0.022
50	0.477	0.037	0.232	0.028	0.8994	0.1349	0.863	0.120	1.058	0.144	0.385	0.045	0.198	0.027	0.097	0.010
60	0.358	0.030	0.219	0.028	0.8079	0.1212	0.672	0.093	0.661	0.089	0.211	0.026	0.153	0.019	0.062	0.006
70	0.295	0.029	0.228	0.028	0.7272	0.1091	0.561	0.077	0.428	0.056	0.153	0.018	0.116	0.017	0.052	0.005
80	0.284	0.034	0.245	0.031	0.6026	0.0904	0.499	0.068	0.322	0.045	0.121	0.017	0.089	0.011	0.038	0.004
90	0.253	0.035	0.260	0.032	0.4794	0.0719	0.443	0.060	0.290	0.039	0.096	0.015	0.081	0.010	0.031	0.003
100	0.247	0.020	0.272	0.034	0.3910	0.0587	0.419	0.003	0.314	0.048	0.094	0.010	0.090	0.011	0.026	0.002
110	0.256	0.036	0.291	0.037	0.2647	0.0397	0.426	0.057	0.409	0.059	0.138	0.020	0.108	0.016	0.026	0.003
120	0.274	0.036	0.334	0.043	0.2523	0.0378	0.517	0.068	0.550	0.081	0.267	0.040	0.127	0.017	0.024	0.002
130	0.286	0.020	0.359	0.045	0.2853	0.0428	0.696	0.092	0.677	0.100	0.40	0.06	0.162	0.019	0.022	0.002
140							0.96	0.14	0.91	0.14	0.70	0.10				

Published by AIP Publishing on behalf of the National Institute of Standards and Technology.

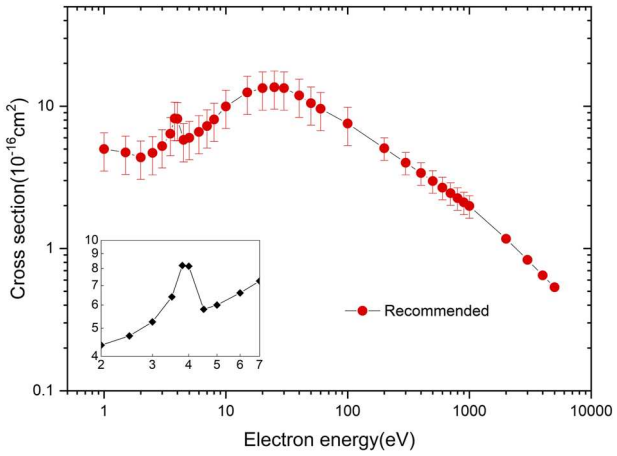

FIG. 5. Recommended elastic integral cross sections of CO_2. The inset shows the resonance region.

measured elastic cross sections seen in Sec. 2.2 also derived MTCSs from their elastic DCS measurements: Register *et al.*,[54] Tanaka *et al.*,[57] Gibson *et al.*,[58] and Iga *et al.*[59] The limitation of the beam-derived MTCSs is that the incident electron energies are typically as low as only 0.1 eV or higher. The lower electron energy region can be covered by the swarm methods. Using this swarm method, Hake and Phelps[65] measured the MTCS of CO_2 in the energy range of 0.01–100 eV, Lowke *et al.*[66] in the energy range 0.07–100 eV, and Nakamura[16] for 0.04–100 eV range. Theoretically, Morrison *et al.*[67] used a coupled-channel investigation of e-CO_2 scattering for incident electron energies from 0.07 to 10.0 eV and presented MTCSs with other cross sections. Takekawa and Itikawa[60] studied elastic scattering of electrons from CO_2 based on an *ab initio* electrostatic potential accounting for approximately effects of electron exchange and target polarization. Alvarez-Pol *et al.*[17] and Gianturco and Stoecklin,[62] respectively, also reported the calculated MTCSs. The recommended MTCS can be derived from the combination of these beam-derived and swarm-derived MTCSs, sometimes with the theoretical calculations also considered. Elford *et al.*[68] recommended a CO_2 MTCS based on that of Nakamura,[16] together with the beam-derived MTCS, in the 0.04–100 eV energy range. In the range from 1 to 20 eV the preferred cross section follows the general form of the Nakamura cross section but with some modifications in the region of the 3.8 eV resonance and at values in the region of 15 eV, see Elford *et al.*[68] The beam-derived cross section values are generally in good agreement with the result of Nakamura. Elford *et al.* estimated the uncertainty limits to be $< \pm 5\%$ for $0.04 \le E < 0.5$ eV, $< \pm 10\%$ for $0.5 \le E < 20$ eV and $< \pm 20\%$ for $20 \le E < 100$ eV, where E indicates the incident electron energy. Itikawa[13] took the recommendation of Elford *et al.* in his recommendation of the cross sections of electron scattering for the energy range from 0.01 to 100 eV. In addition to these recommendation, we can add the beam-derived MTCS of Iga *et al.*[59] from 100 to 400 eV with an uncertainty of 20%. In conclusion, we provide an extended set of recommended MTCSs for CO_2 from 0.01 to 400 eV, with the uncertainties given by Elford *et al.* Recommended MTCSs are given in the Fig. 6 and Table 5.

TABLE 4. Recommended elastic integral cross sections of CO_2

Electron energy (eV)	ICS (10^{-16} cm^2)	Electron energy (eV)	ICS (10^{-16} cm^2)
1.0	5.00	40	11.9
1.5	4.73	50	10.5
2.0	4.37	60	9.6
2.5	4.70	100	7.55
3.0	5.25	200	5.07
3.5	6.40	300	4.01
3.8	8.20	400	3.39
4.0	8.15	500	2.98
4.5	5.80	600	2.68
5.0	6.00	700	2.45
6.0	6.60	800	2.26
7.0	7.25	900	2.11
8.0	8.06	1000	1.99
10	9.95	2000	1.17
15	12.5	3000	0.83
20	13.4	4000	0.65
25	13.6	5000	0.53
30	13.4		

2.4. Rotational excitation cross section

Because the ^{16}O oxygen has zero nuclear spin and the CO_2 ground electronic ground state is $^1\Sigma_g^+$, in the ground vibronic state, the main isotopologue $^{12}C^{16}O_2$ can only have even values of rotational angular momentum quantum number j. The same is true for the $^{12}C^{18}O_2$ isotopologue. The rotational constants of CO_2 are given by Itikawa.[13] For the ground vibronic state of $^{12}C^{16}O_2$, energies of the lowest rotational levels are given by

$$E_{0j} = E_{00} + B_0 j(j+1) - D_0[j(j+1)]^2, \quad (2)$$

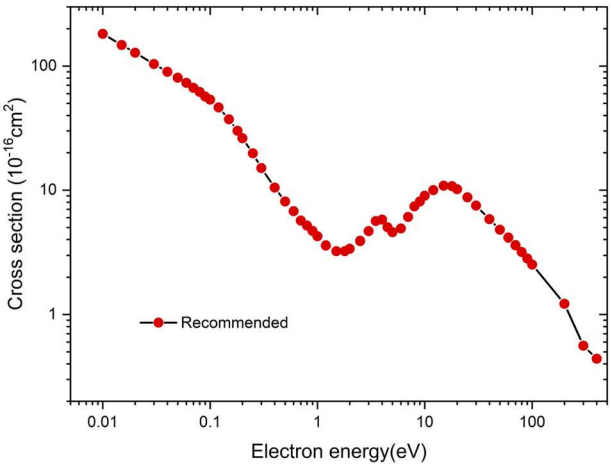

FIG. 6. Recommended elastic MTCSs of CO_2.

Published by AIP Publishing on behalf of the National Institute of Standards and Technology.

TABLE 5. Recommended elastic MTCSs of CO_2. Uncertainties are ±5% for $0.04 \le E < 0.5$ eV, ±10% for $0.5 \le E < 20$ eV and ±20% for $20 \le E < 400$ eV

Electron energy (eV)	MTCS (10^{-16} cm^2)	Electron energy (eV)	MTCS (10^{-16} cm^2)
0.01	182	2.5	3.91
0.015	148	3	4.67
0.02	128	3.5	5.64
0.03	104	4	5.79
0.04	90	4.5	5.02
0.05	80.6	5	4.58
0.06	73.2	6	4.91
0.07	66.8	7	6.08
0.08	61.9	8	7.4
0.09	56.8	9	8.09
0.1	53.6	10	9.02
0.12	46.4	12	10
0.15	37.2	15	10.86
0.18	30.1	18	10.76
0.2	26.2	20	10.17
0.25	19.8	25	8.74
0.3	15.05	30	7.51
0.4	10.48	40	5.84
0.5	8.09	50	4.79
0.6	6.77	60	4.15
0.7	5.69	70	3.61
0.8	5.18	80	3.19
0.9	4.69	90	2.83
1	4.25	100	2.53
1.2	3.59	200	1.22
1.5	3.24	300	0.56
1.8	3.24	400	0.44
2	3.39		

where E_{00} is the energy of the ground rovibronic level of the molecule and the rotational constants B_0 and D_0 are 0.3902 and 1.333×10^{-7} cm^{-1}, respectively.

In previous reviews by Itikawa,[13] Nakamura,[16] and Anzai *et al.*,[15] no data on rotational excitation of CO_2 were discussed. There have been several theoretical studies on rotational excitation of CO_2 by electron impact starting from the ground vibrational level of the molecule. Morrison and Lane[69] used the adiabatic-nuclei-rotational (ANR) approximation, a coupled-channels approach, and the static-exchange model (SE) to the potential representing the interaction of the electron with the molecule. Elastic $j = 0 \rightarrow 0$ and inelastic $j = 0 \rightarrow 2, 4$ cross sections were computed. Later, Thirumalai *et al.*[70] used a static-exchange-plus-polarization (SEP) potential and a coupled-channel approach. In addition, the vibrational motion was accounted for. Unfortunately, the calculations were performed only for one scattering energy, 10 eV. Later, Gianturco and Stoecklin[71] calculated the rotational excitation cross sections starting from $j = 0, 2$, and 4 using an approach very similar to the one by Morrison and Lane:[69] ANR, SE, and the coupled-channel calculations, with a fixed geometry for the target molecule. Elastic and inelastic cross sections for transitions $j \rightarrow j'$ between $j = 0, 2, 4$ and $j' = 0, 2, 4, 6$ were computed for collision energies 2–10 eV. The cross sections from the two studies are reproduced in Fig. 7. While the results are obtained with the ANR approximation, do not account for the vibrational motion, and miss the low-energy region, below 1 eV, in the absence of other reliable data, we recommend the results by Gianturco and Stoecklin,[71] shown in Fig. 8 for transitions from the ground states and the two lowest excited rotational states $j = 0, 2, 4$ to the first four states $j' = 0, 2, 4, 6$.

Cross sections for rotational excitation starting from the lowest excited vibrational levels would also be useful for the plasma modeling community. Such data are not available, although simplified models for e-CO_2 scattering for bending molecule [such as for the (010) vibrational level] were proposed, for example, by Vanroose *et al.*[72] New calculations are clearly needed for rotational excitation of CO_2.

2.5. Vibrational excitation cross section

Vibrational excitation of the CO_2 molecule was considered in several experimental studies by Nakamura,[16] Register *et al.*,[54] Kochem *et al.*,[55] Antoni *et al.*,[73] Kitajima *et al.*,[74] Poparic *et al.*[75] as well as in theoretical ones by Szmytkowski *et al.*,[76] Kazansky and Sergeeva,[77] Kazanskii,[78] Rescigno *et al.*,[79] McCurdy *et al.*,[80] Pietanza *et al.*,[81] Laporta *et al.*[82] Analysis of the vibrational cross sections in CO_2 is particularly difficult due to complex resonance phenomena, including the electronic $^2\Pi_u$ resonance at scattering energy 3.8 eV and the Fermi resonances for excitation dyads and triads of the nearly-degenerate vibrational levels of CO_2, such as the (100) and (020) levels. For a detailed discussion see, for example, the experimental study by Allan[50,83] and theoretical studies by Kazansky and Sergeeva,[77] Kazanskii,[78] Rescigno *et al.*[79]

The data available in literature on excitation of one quantum in each of the three modes are collected and compared in Figs. 9 and 10; numerical values are tabulated in the supplementary material.

In his review, Itikawa[13] has recommended cross sections by Kitajima *et al.*[74] for excitation of the ground vibrational level (000)

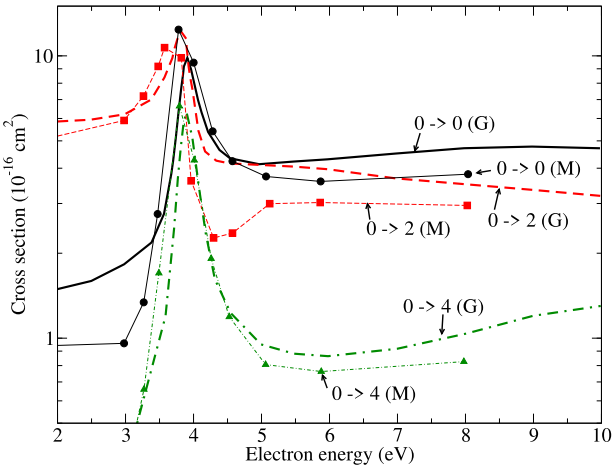

FIG. 7. Comparison of rotational elastic and excitation cross sections obtained by Morrison and Lane[69] (marked with "M") and Gianturco and Stoecklin[71] (marked with "G") for transitions $j = 0 \rightarrow j' = 0, 2, 4$.

Published by AIP Publishing on behalf of the National Institute of Standards and Technology.

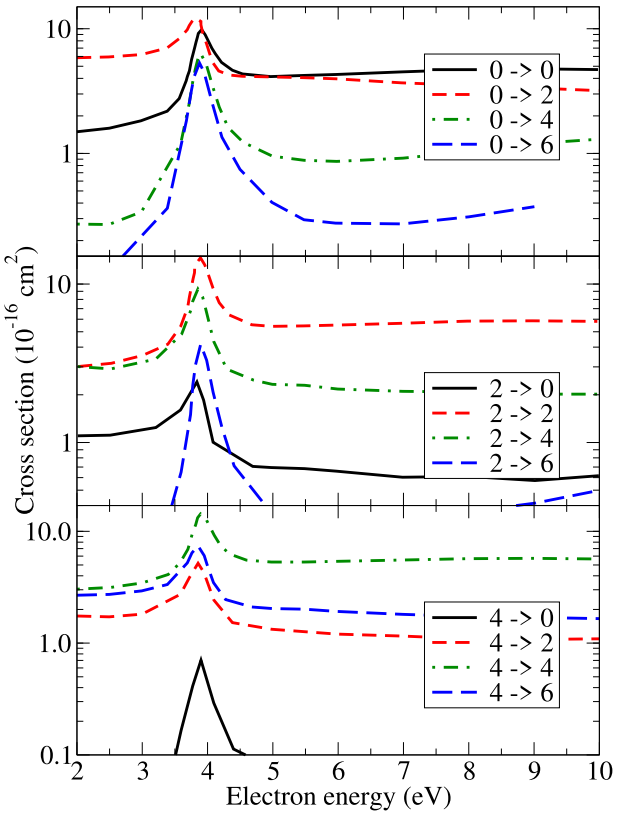

FIG. 8. Cross sections for elastic scattering $j \rightarrow j$ and for rotational (de-)excitation $j \rightarrow j'$ for $j = 0, 2, 4$ and $j' = 0, 2, 4, 6$ obtained by Gianturco and Stoecklin[71] and recommended in this study.

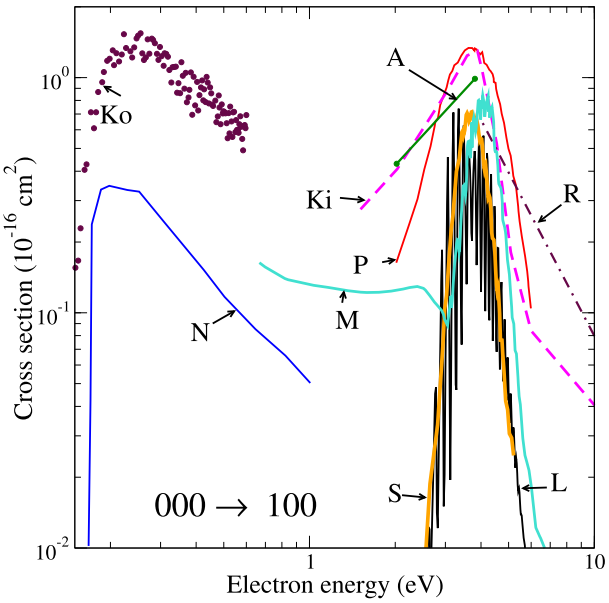

FIG. 9. Cross sections for vibrational excitation of one quantum of the symmetric stretching mode of CO_2 from previous studies. Symbols, making the data, refer to the studies: "A" - Antoni *et al.*,[73] "Ki" - Kitajima *et al.*,[74] "Ko" - Kochem *et al.*,[55] "L" - Laporta *et al.*,[82] "M" - McCurdy *et al.*,[80] "N" - Nakamura,[16] "P" - Poparic *et al.*,[75] "R" - Register *et al.*,[54] "S" - Szmytkowski *et al.*[76]

by one quantum in each mode above 1 eV. At energies below 1 eV, for one-quantum excitation, it was recommended to use the data by Kochem *et al.*[55] for the symmetric mode excitation (000) → (100), and the data by Nakamura[16] for the excitation of the two other modes (000) → (010) and (001).

Since Itikawa's review, there was a beam-electron measurement by Poparic *et al.*[75] of cross sections for excitation of the stretching mode by several quanta. Also theoretical calculations have been performed by Rescigno *et al.*,[79] McCurdy *et al.*[80] for excitation of symmetric stretching and bending modes and by Pietanza *et al.*,[81] Laporta *et al.*[82] for several-quanta excitation for all three modes. All these studies reported cross sections only for energies above 1 eV. No new data are available at lower energies. The data are shown in Figs. 9 and 10.

In their extensive calculations, Laporta *et al.*[82] have reported cross sections for excitation and de-excitation of all three modes by several quanta, obtained using the method of local complex potential, developed for diatomic molecules, separating the modes of CO_2, i.e., in a one-dimensional model for each mode. In this approximation, the inter-mode coupling is neglected, and excitation of two or three modes in a single electron collision is not possible. On the other hand, Rescigno *et al.*[79] and McCurdy *et al.*[80] have argued that due to the Fermi resonance (near-degeneracy of one quantum in the symmetric mode with two quanta in the bending mode), the one-dimensional description of the vibrational dynamics of CO_2 is not accurate. In their study, McCurdy *et al.*[80] have developed a much more accurate model for the process, which includes the two-dimensional dynamics along the two modes (symmetric stretching and bending) and the Renner-Teller coupling between the electronic states of the $CO_2 + e^-$ complex, forming the $^2\Pi_u$ resonance state. The results of their calculations accounting for that complex vibronic resonance are shown in Fig. 9. As one can see, the cross section, obtained in the more accurate 2D approach by Ref. 80 is qualitatively very similar to the 1D calculations by Szmytkowski *et al.*,[76] performed in 1978 and to the more recent calculations by Laporta *et al.*[82] The peak of the resonance in the 2D calculations is shifted slightly to higher energies and the magnitude at the peak is about 10% larger than, for example, in the calculations by Szmytkowski *et al.*[76] When compared to the experimental cross sections by Kitajima *et al.*[74] and Poparic *et al.*,[75] the agreement of the three calculations[76,80,82] is overall quite similar. The experimental cross section is about 70%–100% higher than the calculations near the peak of the resonance.

We note that in the calculations by McCurdy *et al.*[80] and Laporta *et al.*[82] for excitation of the bending and asymmetric stretching modes, only transitions with even numbers of quanta (such as $\Delta v = 2, 4, 6$) were considered. In the early study by Szmytkowski *et al.*,[76] only the symmetric stretching mode was considered. The one-quanta transitions ($\Delta v = 1$) for the bending and asymmetric stretching modes are allowed, if the rotational state of CO_2 changes, but they were not considered in the theoretical studies. This appears to be a significant gap in theory.

Published by AIP Publishing on behalf of the National Institute of Standards and Technology.

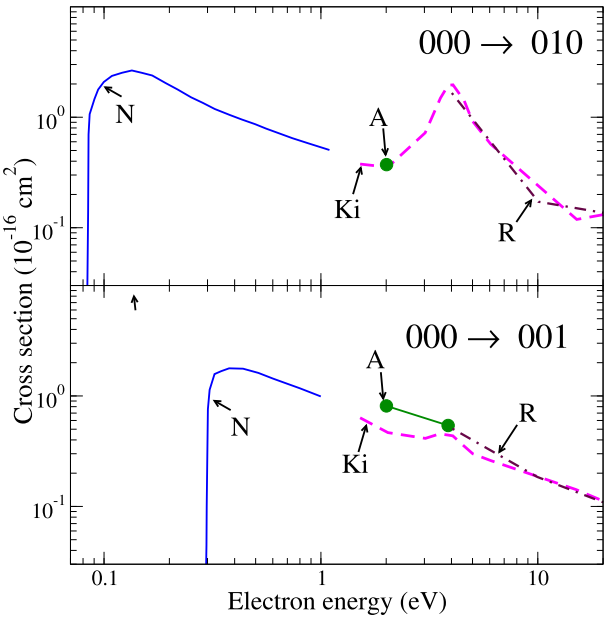

FIG. 10. Cross sections for vibrational excitation of one quantum of the bending (the upper panel) and asymmetric stretching (the lower panel) modes of CO_2 from previous studies. The meaning of the marking symbols is the same as in Fig. 9.

In this review, we recommend the use of the following cross sections for vibrational excitation:

- For the (000) → (100) transition, at energies below 0.6 eV the data by Kochem *et al.*,[55] above 0.6 eV the data by McCurdy *et al.*[80] The uncertainty is probably about 20%.
- For (000) → (010) and (000) → (001) transitions at energies below 1 eV the data by Nakamura,[16] while above 1 eV the data by Kitajima *et al.*[74] The uncertainty is also about 20%.
- No low-energy (below 1 eV) data are recommended for other transitions.
- For the (000) → (*n*00), (0*n*0), and (00*n*) transitions with $n > 1$, for transitions from excited vibrational levels, and for transitions with $\Delta v = 2, 4, 6$, etc. between the levels of the bending and asymmetric stretching modes for energies above 1 eV we recommend to use the data by Laporta *et al.*[82] (available to download as auxiliary data to the original article). For these data, the uncertainty is probably about 40% for not very excited vibrational levels, while at higher energies, the separate-mode approximation, employed in Ref. 82 is not expected to be accurate.
- For transitions with an odd number of excitation quanta for the bending and asymmetric stretching modes and mixed-mode excitation no data are available.

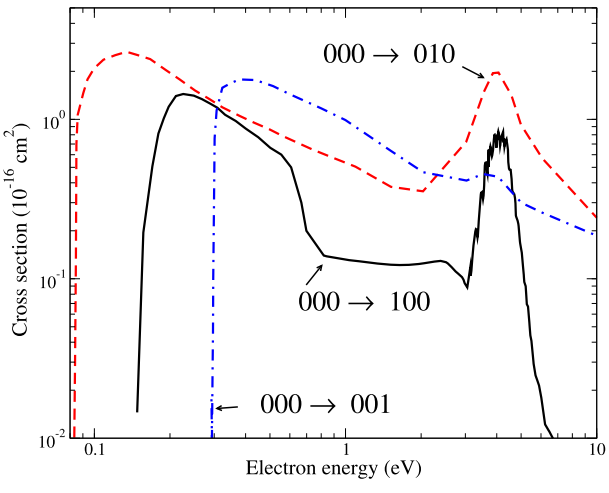

FIG. 11. Recommended cross sections for vibrational excitation from the ground vibrational level by one quantum in each mode. Uncertainty are ±20%. The tabulated values of the shown data are given in the supplementary material.

The recommended cross sections for vibrational excitation from (000) by one quantum in each mode are summarized in Fig. 11. A few example of the cross sections for other transitions are shown in Figs. 12–14.

Concluding this section, we would like to note that accurate calculations of vibrational excitation by one and several quanta at energies below 1 eV are needed. At higher energies, fully-dimensional

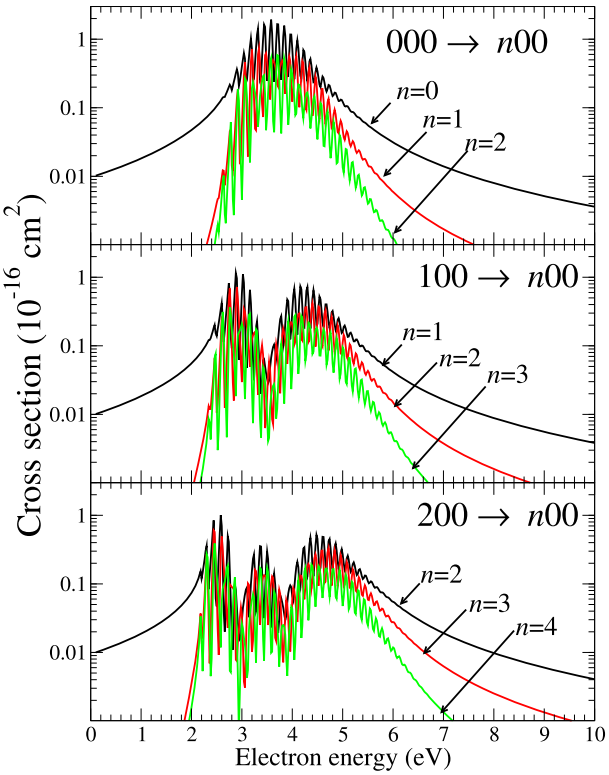

FIG. 12. Cross sections for vibrational excitation of the symmetric stretching mode of CO_2.

Published by AIP Publishing on behalf of the National Institute of Standards and Technology.

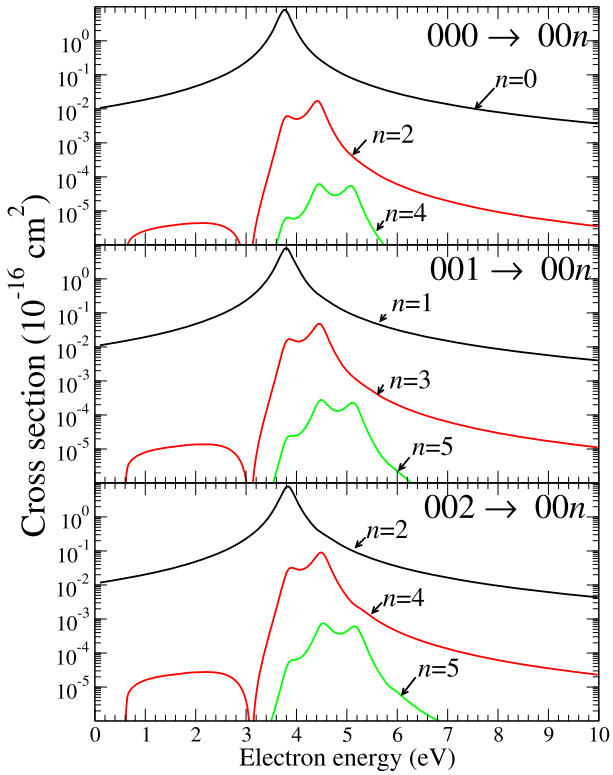

FIG. 13. Cross sections for vibrational excitation of the asymmetric stretching mode of CO_2.

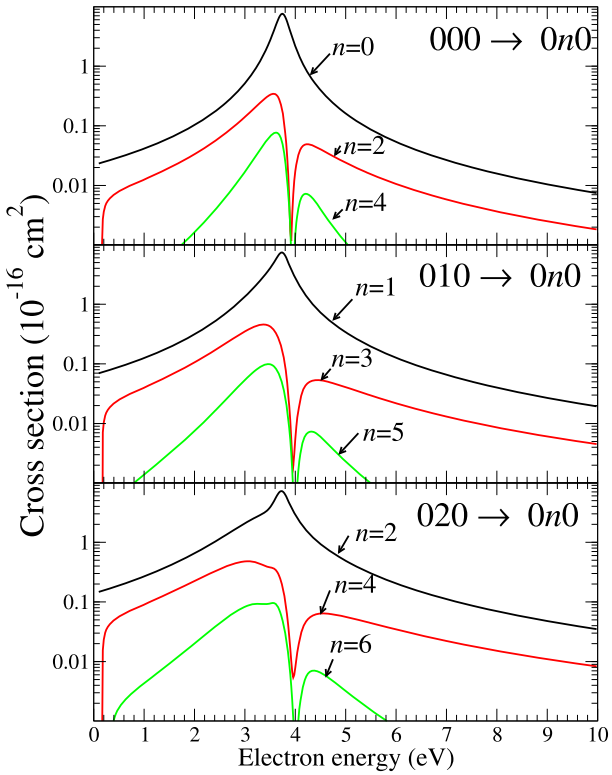

FIG. 14. Cross sections for vibrational excitation of the bending mode of CO_2.

3D calculations would also be desirable, especially, for mixed-mode excitation.

2.6. Electronic excitation cross section

In his comprehensive review Itikawa[13] mentioned the unsatisfactory situation with the data on electronic excitation of CO_2 and did not recommend any data on electronic excitation. In a more recent review, devoted to several molecules, not only to CO_2, Anzai *et al.*[15] recommended cross sections for excitation of the $^1\Sigma_u^+$ (11.048 eV threshold) and $^1\Pi_u$ (11.385 eV threshold) electronic states. These cross section were obtained by Kawahara *et al.*[84] using the Bethe-Born approximation from generalized oscillator strengths (GOS), which – in their turn – were derived from experimental DCSs measured earlier by Green *et al.*[85] In the same study the BE*f*-scaled cross sections were derived from experimental oscillator strengths and theoretical Born-approximation cross sections. The GOS-derived and BE*f*-scaled cross sections for excitation of the $^1\Sigma_u^+$ and $^1\Pi_u$ states agree with each other within ~20%.

In Fig. 15 we show these BE*f*-scaled cross sections[84] for two states dominating the energy-loss spectra (see Fig. 2 in Ref. 85): the $^1\Sigma_u^+$ and $^1\Pi_u$. In contrast to the isoelectronic molecule N_2O, see Figs. 26 and 27 in Ref. 22, the BE*f* model for CO_2 approximates well (within error bars) the experimental values by Kawahara *et al.*[84] who reported data from two laboratories - Flinders and Sophia Universities, and the early high-energy data by Klump and Lassettre,[86] see Fig. 15. The data from the BE*f* model[84] are given in Table 6.

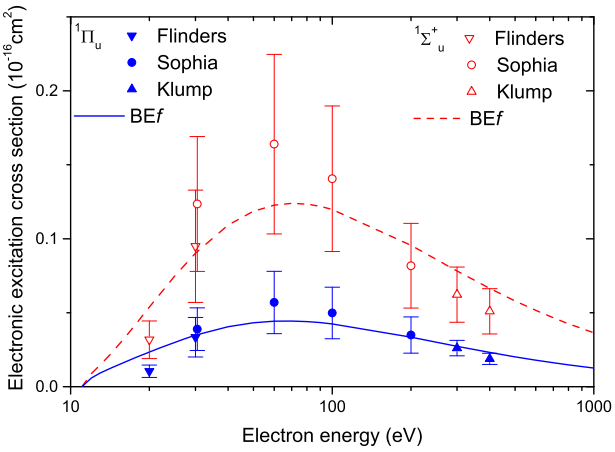

FIG. 15. Cross section for excitation of the $^1\Sigma_u^+$ (broken, red curve and open symbols) and $^1\Pi_u$ (solid, blue curve and closed symbols) electronic states. The Born-scaled BE*f* model[84] is compared with experimental data, from Ref. 84 (Sophia and Flinders Universities) and Ref. 86.

TABLE 6. Recommended cross section for the excitation of the $^1\Sigma_u^+$ and $^1\Pi_u$ electronic states of CO_2. Data are from the Born-scaled BE*f* model[84]

Electron energy (eV)	$^1\Sigma_u^+$ (10^{-16} cm^2)	$^1\Pi_u$ (10^{-16} cm^2)
12	0.0088	0.0058
13	0.0148	0.009 39
14	0.0208	0.0120
15	0.0267	0.0143
16	0.0325	0.0164
17	0.0382	0.0183
18	0.0436	0.0201
19	0.0488	0.0218
20	0.0538	0.0234
25	0.0748	0.0301
30	0.0903	0.0348
40	0.1093	0.0406
50	0.1186	0.0432
60	0.1227	0.0443
70	0.1239	0.0444
80	0.1234	0.0440
90	0.1219	0.0433
100	0.1198	0.0424
200	0.0955	0.0335
300	0.0782	0.0273
400	0.0665	0.0232
500	0.0580	0.0202
600	0.0516	0.0179
700	0.0466	0.0162
800	0.0426	0.0148
1000	0.0364	0.0126
2000	0.0219	0.007 57
3000	0.0160	0.005 53
4000	0.0127	0.004 40
5000	0.0104	0.003 68

For the completeness, we mention also a recent study by Wang and Zhu,[87] in which available experimental oscillator strengths are analyzed and the BE*f*-scaled cross sections for excitation of the $^1\Sigma_u^+$ and $^1\Pi_u$ states are derived in the same way as in the earlier study by Kawahara *et al.*[84] mentioned above.

Quite surprisingly, purely *ab initio* data on integral cross sections for electronic excitation are very scarce.[88–90] The data published in these studies were not recommended by Itikawa.[13]

We note that the lowest-lying electronic excited states of CO_2 are triplets whose excitation cross sections are all zero within the BE*f* model, and the Bethe-Born and BE*f*-scaled cross section are not accurate at low energies, where electronic resonances associated with excited ionization channels closed at a given scattering energy, may play a significant role. As part of this study, therefore we decided to perform new first-principle calculations of cross sections for excitation of the lowest electronic states of CO_2. For these calculations we used the UKRMol suite of codes[91] and the Quantemol-N interface for the code.[92] The calculation were performed for the fixed geometry, corresponding to the CO_2 equilibrium in its ground electronic state. The calculations were performed using the configuration interaction (CI) method with Hartree-Fock orbitals obtained using the `cc-pVTZ` basis set and the Molpro software.[93] In the CI calculations the nine lowest orbitals were frozen, the remaining four electrons in CO_2 were distributed over six orbitals; target states with energies up to 20 eV were kept in the expansion. The 13-bohrs R-matrix radius was used. Because the calculations were performed at a fixed geometry, vibronic effects were not accounted for. It is known that the equilibrium geometry of certain excited states is not linear. Therefore, the present results may not be very accurate. The results are given in Fig. 16.

At 20 eV the sum of the cross sections for presently calculated (optically forbidden) states amounts to about 0.3×10^{-16} cm^2 and for the allowed states, $^1\Sigma_u^+$ and $^1\Pi_u$ the sum[84] is 0.07×10^{-16} cm^2. Altogether this is a factor of two less than the experimental cross section[94] for the dissociation into neutral fragments, see next paragraph.

We note that while we consider excitation to only the eight electronic states for which data are available; above the ionization threshold limit of 13.9 eV, there are an infinite number of open electronic states for which no excitation data are available.

2.7. Neutral dissociation cross section

Dissociation into neutrals is an important reaction channel,[95] particularly in view of possible sequestering carbon from the atmospheric CO_2. Unfortunately, few direct measurements exist. Therefore, in various modeling efforts[19] quite different sets of data are used, including cross sections for dissociative attachment.

Cosby[96] developed a method in which a beam of ions is neutralized in flight, and so obtained the beam of neutral molecules which collides with a beam of electrons. The intrinsic uncertainty of this method is about ±30%. The dissociation of CO_2 was reported by Cosby and Helm[94] in an internal report for Wright and Patterson Co. The maximum of their dissociation cross section is only quarter of the ionization cross section, see Fig. 17 and Table 7. In the case of N_2 the dissociation cross section measured by Cosby[96] amounts at its maximum to as much as half of the ionization cross section, see Fig. 19 in Ref. 10. For CO_2 the primary dissociation channel (>95%) is (CO + O). The dissociation energy of CO_2 is 5.349 eV, but the production of ground state fragments CO($X^1\Sigma^+$) + O (^{3}P) is spin-forbidden from the singlet electronic state in this molecule. Cosby and Helm[94] argued that the dissociation occurs via electronic excitation, leading to excited electronic states of the fragments: CO($X^1\Sigma^+$) + O (^{1}S) (at 9.539 eV) and CO($a^3\Pi$) + O (^{3}P) (at 11.385 eV). From the electron-impact excitation spectrum the expected partitioning into these two channels is 73% and 27%.

Another, to some extent easier method to evaluate the cross section for the dissociation into neutrals is to monitor metastable atoms. This methodology was used by LeClair and McConkey,[97] who studied the production of the metastable (^{1}S) O atoms. As seen from Fig. 17 this cross sections is only approximately one seventh of the cross sections reported by Cosby and Helm.[94] Note that the cross section measured by LeClair and McConkey[97] is frequently quoted as the "total dissociation," which is misleading.

We stress also that the method by Cosby[94,96] may be subject to some systematic uncertainties, like an incomplete collecting of the fragments produced, due to their different velocities. A complementary method would be the study the optical emission of the

Published by AIP Publishing on behalf of the National Institute of Standards and Technology.

dissociated fragments. However, the measured emission cross sections from the O atom (at 130.4 nm) and from the CO fragment (the fourth positive system, i.e., de-excitation of the $A\ ^1\Pi$ state, and the Cameron system, i.e., the de-excitation of the metastable $a\ ^3\Pi$ state) gave cross sections of order 10^{-18} cm^2, see Itikawa[13] for a detailed discussion. Recent experiments[99] on plasmas suggest that the dissociation into neutrals may go mainly through excitation into metastable electronic states rather than via a direct electron impact. In conclusion, we are not able to provide recommended values: the electron impact dissociation into neutrals is an important process that requires further investigations.

2.8. Ionization cross section

TCS for ionization were measured by Asundi *et al.*,[100] Rapp and Englander-Golden,[101] Hudson *et al.*,[102] partial (and total as the sum) cross sections by Straub *et al.*,[98] Adamczyk *et al.*,[103] Adamczyk *et al.*,[104] Crowe and McConkey,[105] Märk and Hille,[106] Tian and Vidal.[107] Only a few of these sets are absolute: Rapp and

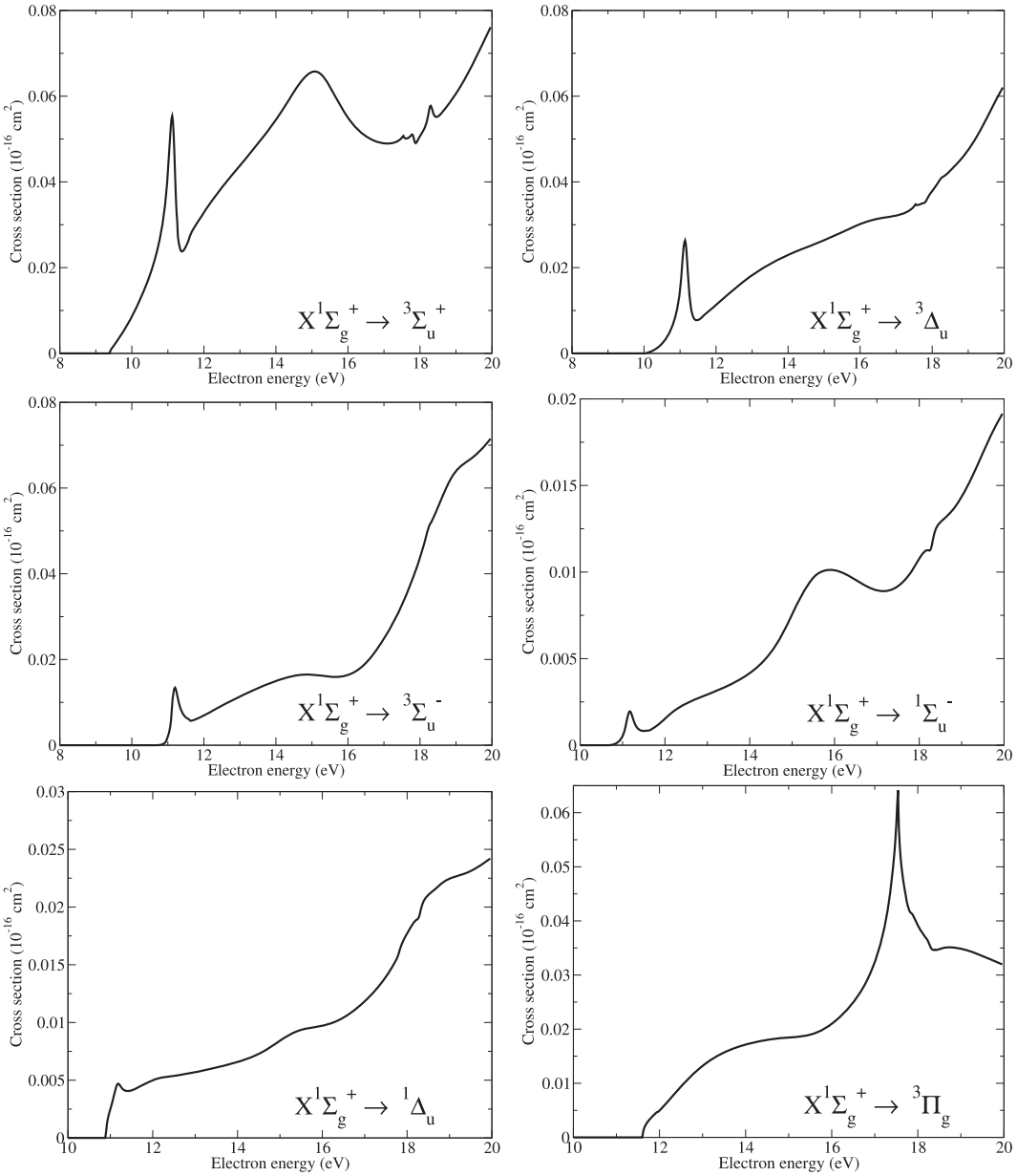

FIG. 16. Cross section for excitation of the electronic state.

Published by AIP Publishing on behalf of the National Institute of Standards and Technology.

TABLE 7. Cross section for the dissociation of CO_2 into neutrals: beam measurements by Cosby and Helm,[94] digitalized from their Fig. 15 (p. 38). The uncertainty on the energy scale is ±1 eV and on the cross section values ±30%

Electron energy (eV)	Dissociation cross section (10^{-16} cm^2)
12.2	0.01
14.9	0.276
18.4	0.439
20.3	0.814
23.3	0.964
27.9	0.956
32.9	0.904
37.9	0.900
43.2	0.776
47.8	0.825
53.2	0.713
58.1	0.765
72.7	0.653
97.1	0.638
147	0.458
197	0.398

Englander-Golden,[101] Straub *et al.*,[98] and Hudson *et al.*[102] measured total ion currents, while Freund *et al.*[108] monitored the flux of the neutral beam (with ±10% uncertainty). Other measurements used normalization procedures: Crowe and McConkey,[105] Adamczyk *et al.*[103] - to the total ionization cross sections by Rapp and Englander-Golden,[101] Orient and Srivastava[109] - to Ar^+ data (±5% estimated error bar), Tian and Vidal[107] normalized to data by Straub *et al.*,[98] and King and Price[110] reported partial cross sections relative to the CO_2^+ ion. The dominant ion is the parent, i.e., the CO_2^+ species, that in its maximum exceeds by a factor of almost ten the cross section for the production of the CO^+ ion, see Fig. 18. Surprisingly, the production of the O^+ exceeds that of CO^+; note also that above 50 eV the yield of the O^+ ion is double that of C^+.

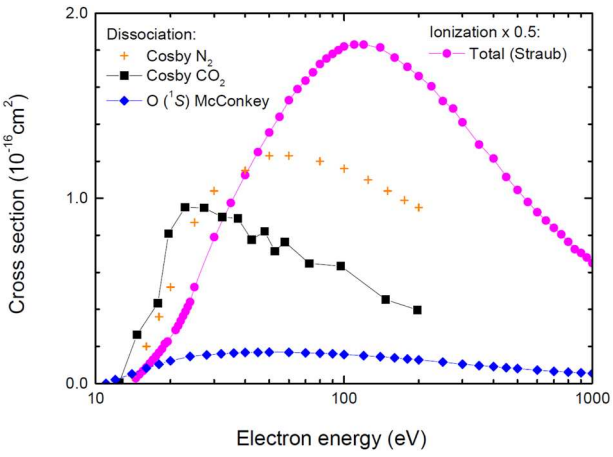

FIG. 17. Evaluation of cross sections for dissociation of CO_2 into neutral fragments. Total dissociation cross section of Cosby and Helm[94] is compared with the total dissociation for N_2 from the same lab.[96] Production of metastable $O(^1S)$ atoms was studied by LeClair and McConkey.[97] For comparison the total ionization cross section in CO_2 measured by Straub *et al.*[98] is also given.

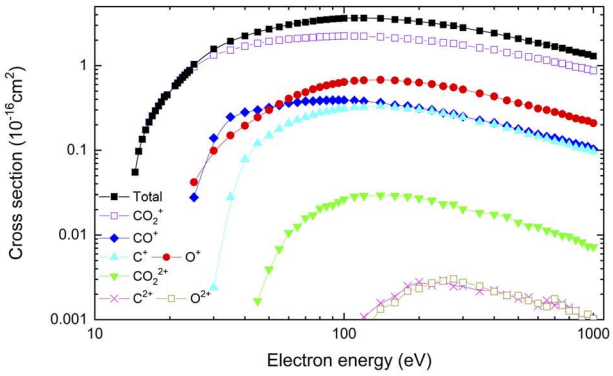

FIG. 18. Partitioning of CO_2 ionization cross section into different ionization fragments: recommended data, based on the review by Lindsay and Mangan.[111]

The agreement between different laboratories is somewhat poorer than in the case of CH_4, see Ref. 20 For the total ionization cross section there are differences in the maximum between all, but those by Orient and Srivastava,[112] is within ±5%, see Fig. 19. The most recent absolute measurements by Hudson *et al.*[102] agree very well in the maximum with earlier data[98,101] but are somewhat lower in the threshold region. The recommended total ionization cross sections lie within two alternative BEB (Binary Encounter Bethe-Born, see Ref. 113) approximations: that using the Hartree-Fock and the Density functional theory (QTP00),[114] form lower and upper bounds, respectively, see Fig. 19 (present calculations, using an aug-cc-pVTZ basis set).

For the CO_2^+ ion the difference in the maximum of the cross section between the recent data is about ±10%, see Fig. 20. The two uppermost measurements on this figure, by Adamczyk *et al.*[104]

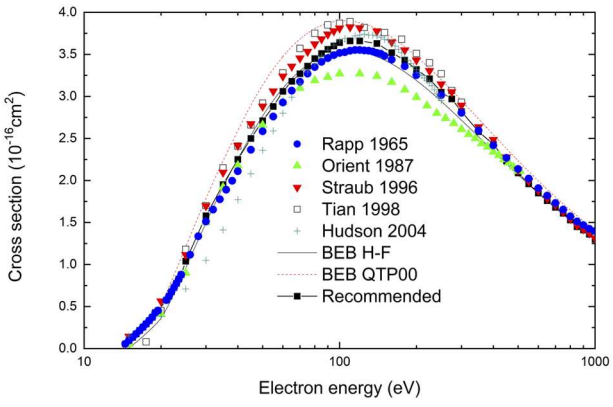

FIG. 19. Total ionization cross section. Experiments are from Straub *et al.*,[98] Rapp and Englander-Golden,[101] Hudson *et al.*,[102] Tian and Vidal,[107] Orient and Strivastava;[112] BEB approximation in Hartree-Fock, and in Density functional theory (QTP00),[114] together with presently recommended values. The recommended values lie within the limits of these two alternative theoretical approximations.

Published by AIP Publishing on behalf of the National Institute of Standards and Technology.

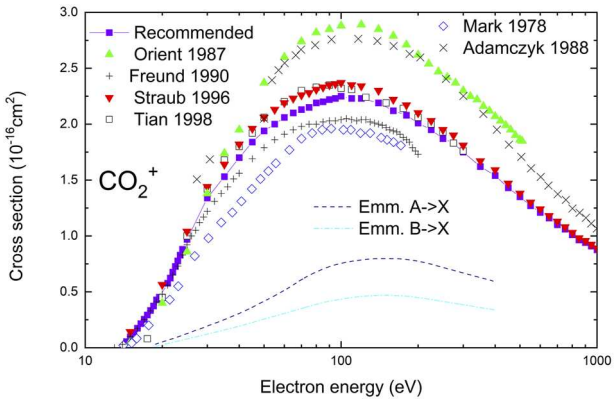

FIG. 20. Partial ionization cross section for the formation of CO_2^+ ion. Experiments are Refs. 98, 104, 106–108, and 112. Not shown are data by Krishnakumar,[115] which practically coincide with those by Orient and Strivastava[112] and by Crowe and McConkey,[105] which are lower than recommended, and close to those by Adamczyk *et al.*,[103] as both sets were normalized to absolute values by Rapp and Englander-Golden.[101] The two lower curves are cross section for the optical emission from excited states of the CO_2^+ ion.[13]

and Orient and Srivastava[109] probably suffered from incomplete collections of the less abundant fragment ions, which, with the normalization adopted, overestimates the CO_2^+ cross section. In the same figure we show cross sections for the optical emission from two excited states of the CO_2^+ ion: at 150 eV about half of the CO_2^+ ions is produced in excited, $A\,^2\Pi_u$ and $B\,^2\Sigma_u^+$ states, see Fig. 20. (Following the discussion by Itikawa,[13] out of the three available measurements, see Refs. 116–118 we report the data by Tsurubuchi and Iwai.[118])

Cross sections for the formation of the CO^+ from different laboratories show a much bigger spread (some ±20% between the more recent sets) than those for the CO_2^+ ion, see Fig. 21. Only the measurements of Straub *et al.*[98] and of King and Price[110] coincide within ±5%. As already said, King and Price[110] reported only relative

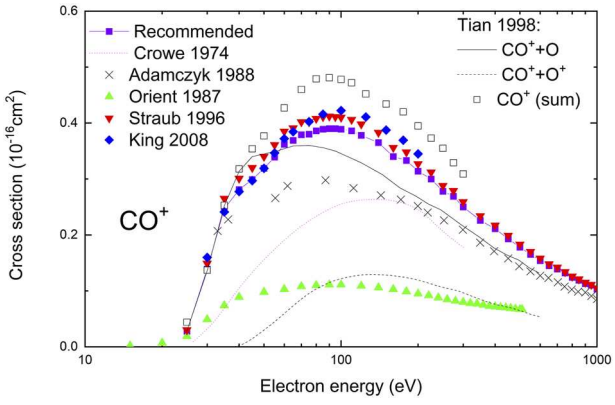

FIG. 21. Partial ionization cross section for the formation of the CO^+ ion. Experiments are by Straub *et al.*,[98] Adamczyk *et al.*,[104] Crowe and McConkey,[105] Tian and Vidal,[107] King and Price,[110] Orient and Strivastava,[112] Tian and Vidal.[119] As indicated by studies of the optical emission,[117] about 1/3 of the CO^+ ion is produced in the excited $B\,^2\Sigma_u^+$ state, see Ref. 13.

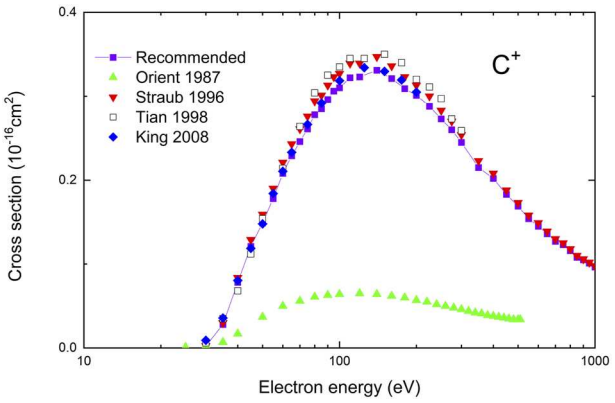

FIG. 22. Partial ionization cross section for the formation of the C^+ ion. Experimental data due to Straub *et al.*,[98] Tian and Vidal,[107] King and Price,[110] Orient and Strivastava.[112]

data: we normalized them to our recommended CO_2^+ cross sections. As shown by coincidence measurements[110,119] the CO^+ ions come, essentially, from two ionization channels. The threshold for the formation of the (CO^+, O) pair is 19.47 eV and for the (CO^+, O^+) pair is 33.08 eV. We show the presence of these two separate channels in Fig. 21, using the data from Ref. 119. At 200 eV the yield of CO^+ from a single ionization channel (i.e., with the O atom production) is higher than that from a double (i.e., CO^+ and O^+) ionization, see Fig. 21. Like the CO_2^+ ion, the CO^+ ion can also be formed in excited states. Optical emission studies[117] show that as much as one third of the CO^+ ion is produced in the $B\,^2\Sigma_u^+$ state, see also Itikawa.[13]

Cross sections for the dissociative ionization into C^+ and O^+ ions are shown in Figs. 22 and 23, respectively. The recent measurements[98,107,110] coincide within ±5%, and only the data by Orient and Strivastava[112] are significantly lower, probably due to systematic differences in the sensitivity of their apparatus to light ions. We note, comparing Fig. 22 with Fig. 23 that the cross section for the formation of the O^+ ion is about twice that of the C^+ ion.

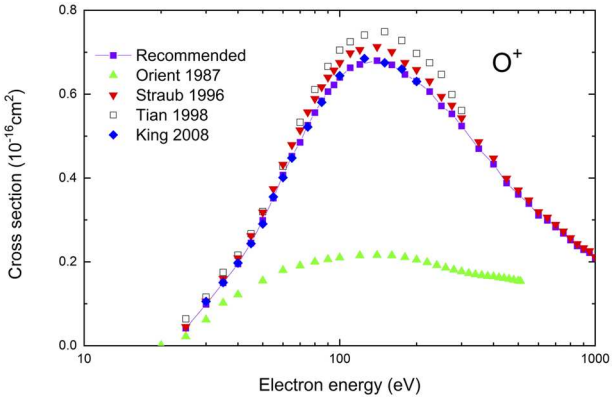

FIG. 23. Partial ionization cross section for the formation of the O^+ ion. Experimental data due to Straub *et al.*,[98] Tian and Vidal,[107] King and Price,[110] Orient and Strivastava.[112]

Published by AIP Publishing on behalf of the National Institute of Standards and Technology.

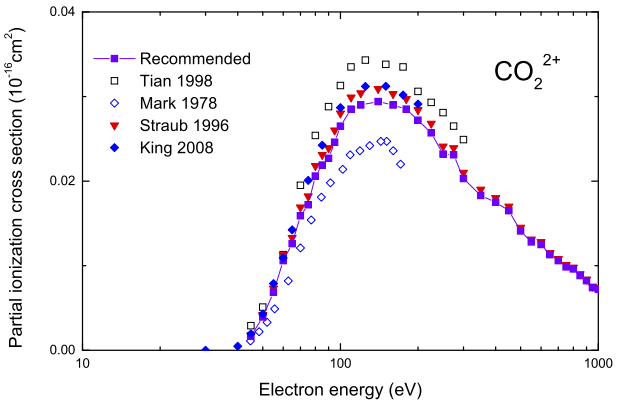

FIG. 24. Partial ionization cross section for the formation of the CO_2^{2+} ion. Experimental data due to Straub *et al.*,[98] Märk and Hille,[106] Tian and Vidal,[107] King and Price.[110]

Cross sections for ionization into doubly charged ions CO_2^{2+}, C^{2+} and O^{2+} are shown in Figs. 24–26 respectively. Again, the most recent measurements[98,107,110] coincide within a few per cent. The cross sections for the formation of the C^{2+} and O^{2+} ions are almost identical in amplitude, each amounting approximately to 0.1% of the total ionization cross section. The cross section for the formation of the CO_2^{2+} ion is by an order of magnitude higher, see Fig. 24. Sharma *et al.*,[120] using a time-of-flight spectrometer, reported a lifetime of 5.6 μs for the CO_2^{2+} ion.

Presently recommended cross sections, see Table 8, are those by Lindsay and Mangan,[111] which in turn are based on absolute measurements by Straub *et al.*[98] The uncertainties[111] in cross sections above 25 eV are ±5% for CO_2^+, CO^+, C^+, O^+ and total ionization. Below 25 eV the uncertainties are ±7% for CO_2^+ and total. The uncertainties for doubly charged ions, CO_2^{2+}, C^{2+}, and O^{2+} are ±6%, ±11%, and ±11%, respectively. Note that the data recommended by Lindsay and Mangan[111] are slightly lower (5% at 100 eV and less than 2% at 1000 eV) than the measurement[98] due to an *ex posteriori* recalibration of their apparatus. Note again, that the data by Straub *et al.*[98] have been confirmed by more recent measurements by Tian and Vidal[107] and King and Price.[110]

The most recent technique, which uses position-sensitive coincidences,[110,121–124] allows the detailed observation of ionization pathways. King and Price[110] reported that at 200 eV the single ionization channel amounts to 81% of the total ion yield, while the double and triple ionization yield was 17.2% and 1.8%, respectively. The same authors gave partial cross sections for CO^+, C^+, O^+ yields via single and double ionization, see Fig. 27 (the data shown are relative to the CO_2^+ cross section). Note that at 200 eV the yield of O^+ from the double ionization reaches that from the single ionization process, while the yield of C^+ from the double ionization is only half of that from the single one.

Bhatt *et al.*[121] at a fixed collision energy of 12 keV reported branching ratios of 65.7%, 9.2%, 16.8% and 6.5% for CO_2^+, CO^+, O^+ and C^+, respectively, not much different from those at 1 keV, see Ref. 98 and 200 eV, see Ref. 110. At the same energy of 12 keV the dominant channels of multiple (double or triple) ionizations are ($O^+ + CO^+$), ($C^+ + O^+ + O$), ($O^+ + O^+ + C$) and ($C^+ + O^+ + O^+$), with relative yields of 44.2%, 33.8%, 12.5% and 5.9%, respectively.[121]

Such detailed data should facilitate better understanding of the ionization processes.

2.9. Dissociative electron attachment cross section

Rapp and Briglia[101] measured the total ion production cross section from CO_2 by dissociative electron attachment process. They obtained two ion peaks: one at 4.3 eV electron energy with the cross section of 1.48×10^{-19} cm^2 and the other at 8.1 eV electron energy with the cross section of 4.28×10^{-19} cm^2. They did not give any uncertainty estimates. Later Orient and Srivastava[109] reported similar results but they measured only O^- ions produced by electron attachment to from CO_2. Their O^- ion peaks appeared, one, at 4.4 eV electron energy with the cross section of 1.43×10^{-19} cm^2 and, the other, at 8.2 eV electron energy with the cross section of 4.48×10^{-19} cm^2. They also observed two very small peaks (cross sections in the range of 10^{-20}–10^{-21} cm^2) at 12.17 and 19 eV. Orient and Srivastava claimed their uncertainty to be about 20%, agreeing with the *total ion* production cross sections of Rapp and Briglia[101] within

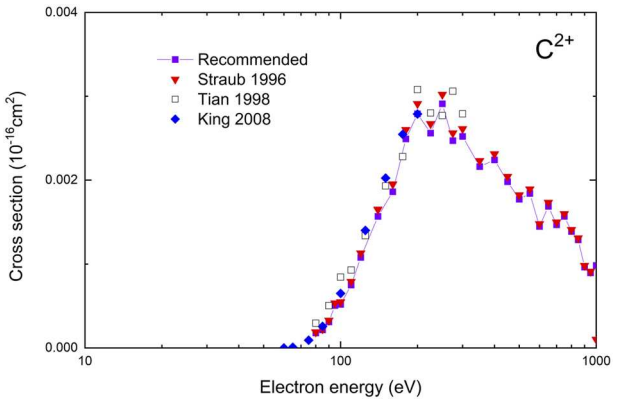

FIG. 25. Partial ionization cross section for the formation of the C^2+ ion. Experimental data due to Straub *et al.*,[98] Tian and Vidal,[107] King and Price.[110]

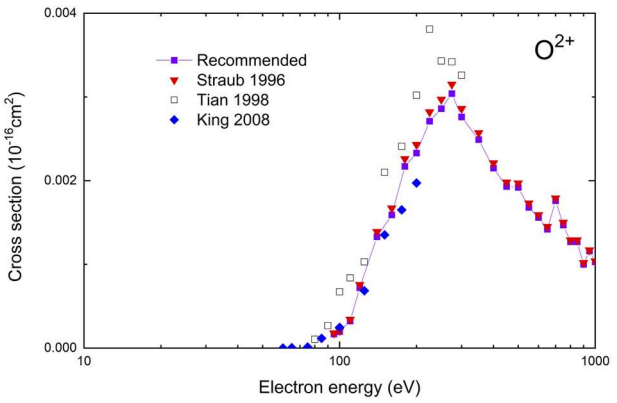

FIG. 26. Partial ionization cross section for the formation of the O^2+ ion. Experimental data due to Straub *et al.*,[98] Tian and Vidal,[107] King and Price.[110]

Published by AIP Publishing on behalf of the National Institute of Standards and Technology.

TABLE 8. Recommended total and partial ionization cross sections for CO_2

Electron energy (eV)	$\sigma(CO_2^+)$ (10^{-16} cm^2)	$\sigma(CO^+)$ (10^{-17} cm^2)	$\sigma(C^+)$ (10^{-17} cm^2)	$\sigma(O^+)$ (10^{-17} cm^2)	$\sigma(CO_2^{2+})$ (10^{-18} cm^2)	$\sigma(C^{2+})$ (10^{-19} cm^2)	$\sigma(O^{2+})$ (10^{-19} cm^2)	σ(total) (10^{-16} cm^2)
14.5	0.055							0.055
15.0	0.097							0.097
15.5	0.135							0.135
16.0	0.174							0.174
16.5	0.215							0.215
17.0	0.255							0.255
17.5	0.293							0.293
18.0	0.333							0.333
18.5	0.373							0.373
19.0	0.428							0.428
19.5	0.452							0.452
21.0	0.577							0.577
21.5	0.623							0.623
22.0	0.676							0.676
22.5	0.727							0.727
23.0	0.777							0.777
23.5	0.828							0.828
24	0.880							0.880
25	0.969	0.279		0.419				1.04
30	1.34	1.39	0.0240	0.986				1.58
35	1.53	2.47	0.280	1.50				1.95
40	1.70	2.81	0.782	1.95				2.25
45	1.84	2.99	1.21	2.45	0.166			2.50
50	1.94	3.19	1.49	2.99	0.393			2.71
55	2.00	3.39	1.78	3.52	0.686			2.88
60	2.06	3.62	2.08	4.07	1.06			3.06
65	2.10	3.69	2.29	4.52	1.26			3.18
70	2.13	3.79	2.46	4.85	1.59			3.27
75	2.15	3.80	2.61	5.26	1.72			3.36
80	2.19	3.86	2.78	5.56	2.06	0.179		3.45
85	2.20	3.89	2.85	5.84	2.19	0.215		3.51
90	2.22	3.90	2.96	6.06	2.27	0.311		3.56
95	2.23	3.90	3.06	6.22	2.46	0.506	0.169	3.60
100	2.25	3.89	3.10	6.40	2.65	0.520	0.197	3.64
110	2.23	3.86	3.22	6.63	2.85	0.751	0.324	3.66
120	2.23	3.78	3.23	6.71	2.90	1.08	0.721	3.66
140	2.19	3.65	3.31	6.80	2.94	1.57	1.33	3.63
160	2.12	3.40	3.21	6.70	2.90	1.86	1.59	3.52
180	2.08	3.33	3.09	6.47	2.85	2.49	2.17	3.43
200	2.01	3.14	3.01	6.31	2.72	2.79	2.33	3.32
225	1.95	3.00	2.88	6.06	2.57	2.56	2.71	3.21
250	1.87	2.78	2.73	5.72	2.32	2.91	2.86	3.05
275	1.83	2.69	2.60	5.53	2.31	2.47	3.04	2.97
300	1.75	2.50	2.45	5.24	2.03	2.52	2.76	2.82
350	1.62	2.26	2.15	4.70	1.83	2.16	2.49	2.58
400	1.54	2.11	2.02	4.33	1.75	2.24	2.15	2.43
450	1.43	1.93	1.83	3.88	1.65	1.98	1.93	2.23
500	1.35	1.78	1.69	3.61	1.41	1.77	1.92	2.09
550	1.27	1.65	1.54	3.39	1.28	1.84	1.68	1.96
600	1.21	1.54	1.45	3.11	1.25	1.45	1.56	1.85
650	1.16	1.45	1.36	2.99	1.13	1.69	1.42	1.76
700	1.10	1.39	1.27	2.83	1.06	1.47	1.76	1.68
750	1.06	1.32	1.23	2.68	0.986	1.57	1.47	1.61

Published by AIP Publishing on behalf of the National Institute of Standards and Technology.

TABLE 8. (*Continued*)

Electron energy (eV)	$\sigma(CO_2^+)$ (10^{-16} cm^2)	$\sigma(CO^+)$ (10^{-17} cm^2)	$\sigma(C^+)$ (10^{-17} cm^2)	$\sigma(O^+)$ (10^{-17} cm^2)	$\sigma(CO_2^{2+})$ (10^{-18} cm^2)	$\sigma(C^{2+})$ (10^{-19} cm^2)	$\sigma(O^{2+})$ (10^{-19} cm^2)	σ(total) (10^{-16} cm^2)
800	1.01	1.24	1.16	2.52	0.961	1.39	1.27	1.53
850	0.964	1.19	1.08	2.38	0.883	1.29	1.27	1.45
900	0.941	1.13	1.05	2.29	0.823	0.965	1.00	1.41
950	0.909	1.10	1.01	2.22	0.741	0.897	1.16	1.36
1000	0.876	1.03	0.964	2.09	0.723	0.984	1.03	1.30

the uncertainty limit. In 1974, Spence and Schulz[125] also noticed C^- and O_2^- ions produced from CO_2, but with an extremely small cross sections in the range of 10^{-21} and 10^{-24} cm^2, respectively.

Therefore, even though Rapp and Briglia measured total ions, the contributions from ions other than O^- must be negligibly small, which means their cross sections cited above are practically the cross sections for O^- ion production. It was suggested that the lower-energy peak is associated with the $^2\Pi_u$ shape resonance and that the high-energy peak is, it is associated with an electronically excited $^2\Pi_g$ Feshbach-type resonance.[126] The recent relative measurements by Lozano *et al.*[33] give relative peak heights in good agreement with our recommended values.

In recommending the cross sections of either Rapp and Briglia[101] or Orient and Srivastava,[109] each one has a problem; Rapp and Briglia presented the numerical values of their cross section in the tabulated form but no uncertainty was given, while Orient and Srivastava gave their data only in the graphical form but presented 20% of the uncertainty. Since digitizing the graph would result in an additional error, we recommend the numerical values of Rapp and Briglia, and we could estimate that their uncertainty may not be over 20% based on the experiments of Orient and Srivasta and on other ionization experiments in general. Recommended DEA cross sections are given in the Fig. 28 and Table 9.

3. CO_2^+ Ion

Knowledge of cross sections involving CO_2^+ cations is essential for modeling the chemistry of plasmas used for the conversion of CO_2 into carbon-neutral fuels.[127] The dissociative recombination of the CO_2^+ ions with free electrons is probably the source of oxygen atoms in the atmosphere of Mars.[128,129]

3.1. Dissociative recombination cross section

The recombination of the CO_2^+ ion with slow electrons leads to dissociation of the formed neutral molecule. The kinetics of the reaction allows two fragmentation channels: (C + O_2) and (CO + O) with the excess energy of 2.3 and 8.3 eV, respectively.[130,131] The most recent experiment by Viggiano *et al.*[131] in the CRYRING storage ring, in contrast to the earlier measurements by Seiersen *et al.*[130] in the ASTRID ring, confirmed only the dissociation via the (CO + O) channel.

The data from the storage-ring experiments[130,131] mentioned above are shown in Fig. 29. Usually, in this type of experiments, the rate constant - rather than the cross section - is reported, due to the fact that measurements are made with a non-thermal distribution over scattering energies. To obtain the cross section, the reported rate constant should be divided with the velocity corresponding the difference in relative velocities of ions and electrons averaged over the distribution. This velocity, while is an average, is

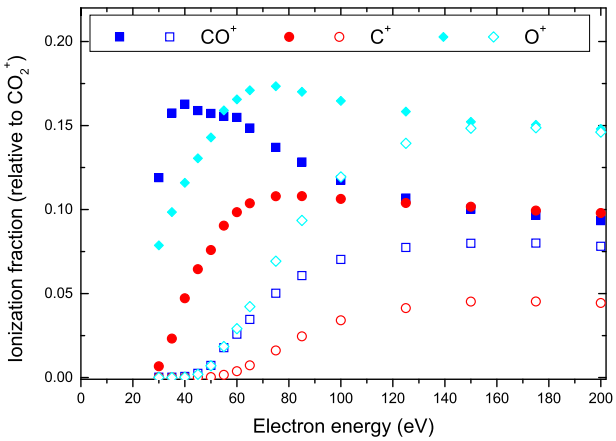

FIG. 27. Cross sections for single and double ionization, relative to the CO_2^+ yield, from King and Price.[110] Closed symbols - single ionization, open symbols - double ionization.

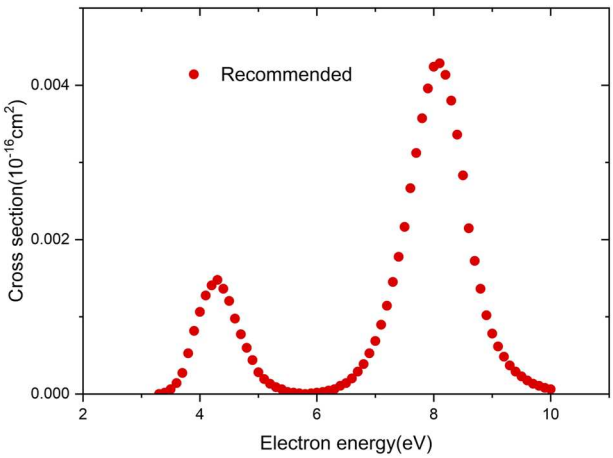

FIG. 28. Recommended dissociative electron attachment cross sections for CO_2.

Published by AIP Publishing on behalf of the National Institute of Standards and Technology.

TABLE 9. Recommended dissociative attachment cross section for CO_2

Electron energy (eV)	DEA (10^{-16} cm^2)	Electron energy (eV)	DEA (10^{-16} cm^2)
3.3	0	6.7	2.90×10^{-4}
3.4	1.76×10^{-5}	6.8	3.87×10^{-4}
3.5	6.16×10^{-5}	6.9	5.28×10^{-4}
3.6	1.41×10^{-4}	7.0	6.86×10^{-4}
3.7	2.73×10^{-4}	7.1	8.97×10^{-4}
3.8	5.28×10^{-4}	7.2	0.001 14
3.9	8.18×10^{-4}	7.3	0.001 45
4.0	0.001 06	7.4	0.001 78
4.1	0.001 28	7.5	0.002 16
4.2	0.001 41	7.6	0.002 67
4.3	0.001 48	7.7	0.003 12
4.4	0.001 36	7.8	0.003 57
4.5	0.001 21	7.9	0.003 96
4.6	9.76×10^{-4}	8.0	0.004 24
4.7	7.74×10^{-4}	8.1	0.004 28
4.8	5.98×10^{-4}	8.2	0.004 13
4.9	4.40×10^{-4}	8.3	0.0038
5.0	2.82×10^{-4}	8.4	0.003 36
5.1	1.94×10^{-4}	8.5	0.002 83
5.2	1.32×10^{-4}	8.6	0.002 15
5.3	8.80×10^{-5}	8.7	0.001 72
5.4	6.16×10^{-5}	8.8	0.001 36
5.5	2.64×10^{-5}	8.9	0.001 02
5.6	1.76×10^{-5}	9.0	7.83×10^{-4}
5.7	8.80×10^{-6}	9.1	6.16×10^{-4}
5.8	0	9.2	4.84×10^{-4}
5.9	8.80×10^{-6}	9.3	3.69×10^{-4}
6.0	1.76×10^{-5}	9.4	2.90×10^{-4}
6.1	2.64×10^{-5}	9.5	2.29×10^{-4}
6.2	4.40×10^{-5}	9.6	1.76×10^{-4}
6.3	6.16×10^{-5}	9.7	1.32×10^{-4}
6.4	1.06×10^{-4}	9.8	1.06×10^{-4}
6.5	1.41×10^{-4}	9.9	7.92×10^{-5}
6.6	2.02×10^{-4}	10	6.16×10^{-5}

converted to the energy, which represents approximately the scattering energy. Figure 29 gives the cross sections (y-axis) vs scattering energy (x-axis), obtained in this way from the experimental[130,131] rate constants.

At energies between 0.003 and 0.3 eV, the data from the two experiments agree with each other. Below 0.003 eV the results from CRYRING[131] are higher than that from ASTRID,[130] due to a better energy resolution in energy of electrons in the CRYRING experiment. Above 0.3 eV, the ASTRID data are more reliable. Therefore, it is recommended to use the CRYRING data for energies below 0.3 eV and the ASTRID data above 0.3 eV. The recommended cross section is also shown in Fig. 29.

Convoluted with a thermal velocity distribution, the data from the two experiments produce similar thermally-averaged rate constants as a function of temperature. T, namely

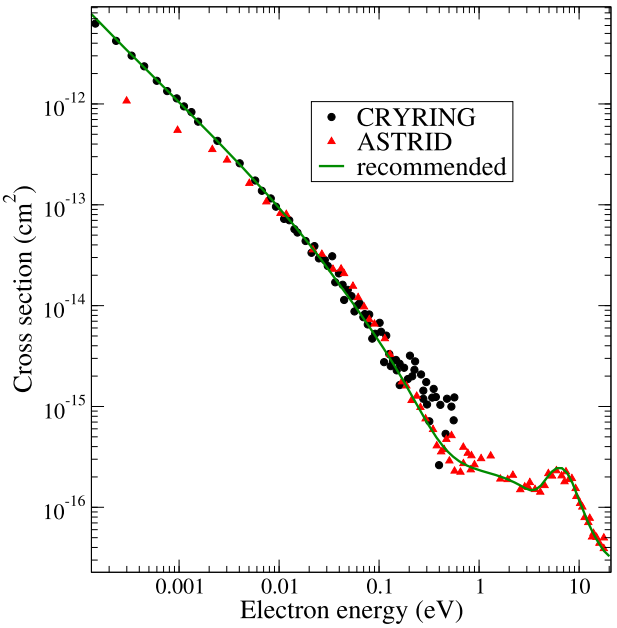

FIG. 29. Cross sections for dissociative recombination of CO_2^+ measured in CRYRING[130] (circles) and ASTRID[131] storage rings. The cross sections are derived from the rate constants reported in the studies. The line represents the recommended data.

$4.2 \times 10^{-7}(T/300)^{-0.75}$, and $6.5(\pm 1.9) \times 10^{-7}(T/300)^{-0.8}$ cm^3/s, respectively. The value reported by Viggiano *et al.*[131] agrees well with the rates for 300 K from the microwave afterglow by Weller and Biondi,[132] and Gutcheck and Zipf,[133] $3.8(\pm 0.5) \times 10^{-7}$ and $4.0(\pm 0.5) \times 10^{-7}$ cm^3/s, respectively, and from flowing afterglow by Geoghegan *et al.*,[134] and Gougousi *et al.*,[135] $3.1(\pm 0.6) \times 10^{-7}$ and $3.5(\pm 0.5) \times 10^{-7}$ cm^3/s, respectively.

Seiersen *et al.*[130] measured on the ASTRID ring also the recombination of the CO_2^{2+} dication, reporting the rate value of $6.2(\pm 2.1) \times 10^{-7}(T_e/300)^{-0.5}$ cm^3/s. They argued, that this result is significant for predicting a CO_2^{2+} ion layer in the atmosphere of Mars.

3.2. Ionization and dissociation cross section

Ionization of the CO_2^+ ion was measured by Müller *et al.*[136] (only for the production of CO_2^{2+} ions) and Bahati *et al.*[137] (who detected CO_2^{2+}, C^+ and O^+ ions), see Fig. 30. For the CO_2^{2+} the two experiments agree within their error bars. The formation of CO_2^{2+} amounts[137] in its maximum to 0.48×10^{-16} cm^2, so it is a factor of ten higher than the direct formation of the CO_2^{2+} ion from CO_2, compare with Fig. 24.

The formation of C^+ and O^+ ions may occur via both electron impact ionization and dissociation. For example, the detection of O^+ ion via ionization may come in coincidence with CO^+, or with ((O^+ + C), with (C^+ + O); and via dissociation with the CO fragment, see Bahati *et al.*,[137] Deutsch *et al.*[138] for details. Unfortunately, the experiments[136,137] did not resolve these particular channels. Note the broad, double-peaked maxima for the production of O^+ and C^+, indicating more than one channel is involved. Measurements

Published by AIP Publishing on behalf of the National Institute of Standards and Technology.

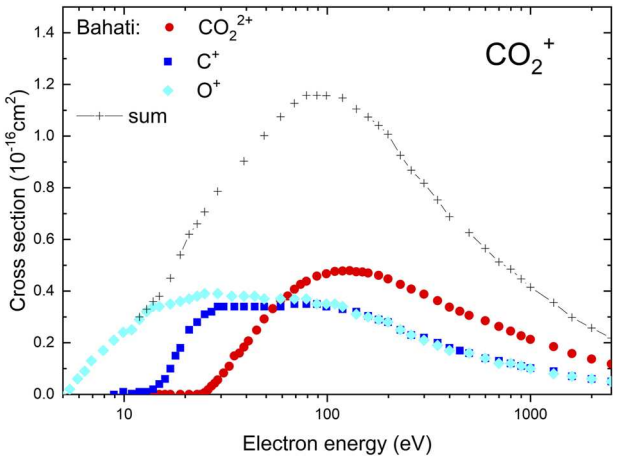

FIG. 30. Formation of ions from the CO_2^+ cation: the CO_2^{2+} comes from the ionization, the O^+ and C^+ ions may be produced both via dissociation (note lower thresholds) and as a result of ionization. The experiment is by Bahati *et al.*[137] The theory by Deutsch *et al.*[138] (not shown) is a factor of two higher that the sum of ions detected experimentally.

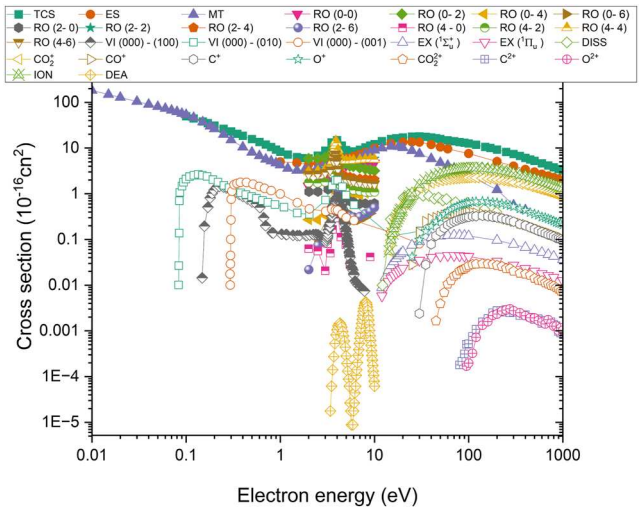

FIG. 31. Summary of recommended cross section for electron collisions with CO_2. TCS - total scattering, ES - elastic scattering, MT - momentum transfer, ION - ionization, VE - vibrational excitation, RO - rotational excitation, EX - electronic excitation, DISS - neutral dissociation, DEA - dissocative electron attachment.

in coincidence, like those of King and Price[110] for CO_2, would be welcome to resolve this issue.

Deutsch *et al.*[138] calculated the total ionization of the CO_2^+ ion; according to them the cross section reaches maximum of about 2×10^{-16} cm^2. This is by a factor of two higher than the sum of the processes measured by Bahati *et al.*,[137] see Fig. 30. Deutsch *et al.*[138] argued that this discrepancy comes from incomplete detection of all possible fragmentation channels of the CO_2^+ ion. However, the threshold for the ionization in the model of Deutsch *et al.*[138] is that for the production of the CO_2^{2+} ion: clearly, the model does not hold for the dissociation and/or dissociative excitation channels. An alternative would be to use the BEB model for ions by Kim *et al.*,[139] but they applied it only for H_2^+, N_2^+, CD^+ and CO^+.

Dynamics and patterns of CO_2^{q+} ions fragmentation, with q = 2, 3, have been studied via electron scattering on CO_2 both experimentally[120,122,124] and theoretically.[120]

4. Summary and Future Work

We reviewed available cross sections resulting from electron collisions with carbon dioxide with aim of compiling a complete dataset of cross sections for plasma and other application. We obtained and are able to recommend an extensive set of electron-scattering cross sections for the CO_2 molecule, as summarized in Fig. 31.

Our recommendations include cross sections for total, elastic, momentum transfer, vibrational and rotational excitations, dissociative electron attachment, electronic levels excitation, ionization, dissociation into neutral fragments via electron scattering; while for the CO_2 ion dissociative recombination cross sections are also reviewed. However, the current interest in plasmas involving CO_2, particularly those aimed at CO_2 valorization, requires cross sections for electron collisions with CO_2 in vibrationally excited states. This is also because relatively long-lived vibrationally excited states may efficiently transfer energy to other molecular species in atmosphere. Such data is largely unavailable. Similarly, cross sections for reactions involving the CO_2^+ (and other ions) need further studies.

5. Supplementary Material

See supplementary material for recommendations on a broad set of electron scattering cross-sections for CO_2 molecules. Data is formatted in Excel format with one process per sheet. The first row of each sheet describes the scattering cross section process of molecules due to electron collisions.

6. Acknowledgments

This research was partially supported by the R & D Program Plasma Big Data ICT Convergence Technology Research Project through the Korea Institute of Fusion Energy (KFE) funded by the Ministry of Science and Technology Information and Communication, Republic of Korea (EN2442). It was also partially funded by the Korea Meteorological Administration Research and Development Program under Grant No. RS-2022-KM221513 and the U.S. National Science Foundation, Grants Nos. 2110279 and 2102188.

7. Author Declarations

7.1. Conflict of Interest

The authors have no conflicts to disclose.

8. Data availability

We provide the recommended dataset as supplementary material. Also numerical data corresponding to the figures are available can be obtained from the corresponding author.

Published by AIP Publishing on behalf of the National Institute of Standards and Technology.

9. References

[1]A. Bogaerts and G. Centi, "Plasma technology for CO_2 conversion: A personal perspective on prospects and gaps," Front. Energy Res. **8**, 111 (2020).

[2]G. Centi, S. Perathoner, and G. Papanikolaou, "Plasma assisted CO_2 splitting to carbon and oxygen: A concept review analysis," J. CO_2 Utiliz. **54**, 101775 (2021).

[3]L. D. Pietanza, G. Colonna, and M. Capitelli, "Self-consistent state-to-state kinetic modeling of CO_2 cold plasmas: Insights on the role of electronically excited states," Plasma Chem. Plasma Process. **44**, 1431 (2023).

[4]S. Ullah, Y. Gao, L. Dou, Y. Liu, T. Shao, Y. Yang, and A. B. Murphy, "Recent trends in plasma-assisted CO_2 methanation: A critical review of recent studies," Plasma Chem. Plasma Process. **43**, 1335–1383 (2023).

[5]J. Dvořák, M. Rankovič, K. Houfek, P. Nag, R. Čurík, J. Fedor, and M. Čížek, "Vibrational excitation in the e + CO_2 system: Analysis of the two-dimensional energy-loss spectrum," Phys. Rev. A **106**, 062807 (2022).

[6]G. V. Naidis and N. Y. Babaeva, "Modeling of vibrational excitation dynamics in a nanosecond CO_2 discharge," J. Phys. D: Appl. Phys. **56**, 015202 (2023).

[7]C. B. Moore, R. E. Wood, B. Hu, and J. T. Yardley, "Vibrational energy transfer in CO_2 lasers," J. Chem. Phys. **46**, 4222–4231 (1967).

[8]C. Fromentin, T. Silva, T. C. Dias, E. Baratte, O. Guaitella, and V. Guerra, "Validation of non-equilibrium kinetics in CO_2–N_2 plasmas," Plasma Sources Sci. Technol. **32**, 054004 (2023).

[9]G. Colonna, M. Capitelli, S. Debenedictis, C. Gorse, and F. Paniccia, "Electron energy distribution functions in CO_2 laser mixture: The effects of second kind collisions from metastable electronic states," Contrib. Plasma Phys. **31**, 575–579 (1991).

[10]M.-Y. Song, H. Cho, G. P. Karwasz, V. Kokoouline, and J. Tennyson, "Cross sections for electron collisions with N_2, N_2^*, and N_2^+," J. Phys. Chem. Ref. Data **52**, 023104 (2023).

[11]S. Kelly, C. Verheyen, A. Cowley, and A. Bogaerts, "Producing oxygen and fertilizer with the Martian atmosphere by using microwave plasma," Chem **8**, 2797–2816 (2022).

[12]G. P. Karwasz, R. S. Brusa, and A. Zecca, "One century of experiments on electron-atom and molecule scattering: A critical review of integral cross-sections. II. Polyatomic molecules," Riv. Nuovo Cimento **24**, 1–118 (2001).

[13]Y. Itikawa, "Cross sections for electron collisions with carbon dioxide," J. Phys. Chem. Ref. Data **31**, 749–767 (2002).

[14]T. Shirai, T. Tabata, and H. Tawara, "Analitic cross secitons for electron collisions with CO, CO_2, and H_2O relevant to edge plasma impurities," At. Data Nucl. Data Tables **79**, 143–184 (2001).

[15]K. Anzai, H. Kato, M. Hoshino, H. Tanaka, Y. Itikawa, L. Campbell, M. J. Brunger, S. J. Buckman, H. Cho, F. Blanco, G. García, P. Limão-Vieira, and O. Ingólfsson, "Cross section data sets for electron collisions with H_2, O_2, CO, CO_2, N_2O and H_2O," Eur. Phys. J. D **66**, 36 (2012).

[16]Y. Nakamura, "Drift velocity and longitudinal diffusion coefficient of electrons in CO_2-Ar mixtures and electron collision cross sections for CO_2 molecules," Aust. J. Phys. **48**, 357–364 (1995).

[17]H. Alvarez-Pol, I. Duran, and R. Lorenzo, "On the cross section of low-energy electron collisions on CH_4 and CO_2," J. Phys. B: At., Mol. Opt. Phys. **30**, 2455 (1997).

[18]T. Wróblewski, G. P. Karwasz, H. Nowakowska, J. Mechlińska-Drewko, V. T. Novaković, and Z. L. Petrović, "Semiempirical analysis of electron scattering cross sections in N_2O and CO_2," Czech J. Phys. **54**, C742–C746 (2004).

[19]M. Grofulović, L. L. Alves, and V. Guerra, "Electron-neutral scattering cross sections for CO_2: A complete and consistent set and an assessment of dissociation," J. Phys. D: Appl. Phys. **49**, 395207 (2016).

[20]M.-Y. Song, J.-S. Yoon, H. Cho, Y. Itikawa, G. P. Karwasz, V. Kokoouline, Y. Nakamura, and J. Tennyson, "Cross sections for electron collisions with methane," J. Phys. Chem. Ref. Data **44**, 023101 (2015).

[21]M.-Y. Song, J.-S. Yoon, H. Cho, G. P. Karwasz, V. Kokoouline, Y. Nakamura, and J. Tennyson, "Cross sections for electron collisions with acetylene," J. Phys. Chem. Ref. Data **46**, 013106 (2017).

[22]M.-Y. Song, J.-S. Yoon, H. Cho, G. P. Karwasz, V. Kokoouline, Y. Nakamura, and J. Tennyson, "Electron collision cross sections with NO, N_2O and NO_2," J. Phys. Chem. Ref. Data **48**, 043104 (2019).

[23]M.-Y. Song, H. Cho, G. P. Karwasz, V. Kokoouline, Y. Nakamura, J. Tennyson, A. Faure, N. J. Mason, and Y. Itikawa, "Cross sections for electron collisions with H_2O," J. Phys. Chem. Ref. Data **50**, 023103 (2021).

[24]K. R. Hoffman, M. S. Dababneh, Y.-F. Hsieh, W. E. Kauppila, V. Pol, J. H. Smart, and T. S. Stein, "Total-cross-section measurements for positrons and electrons colliding with H_2, N_2, and CO_2," Phys. Rev. A **25**, 1393 (1982).

[25]C. K. Kwan, Y. F. Hsieh, W. E. Kauppila, S. J. Smith, T. S. Stein, M. N. Uddin, and M. S. Dababneh, "$e^{\pm}$-CO, $e^{\pm}$-CO_2 total cross-section measurements," Phys. Rev. A **27**, 1328–1336 (1983).

[26]O. Sueoka and S. Mori, "Total cross sections for positrons and electrons colliding with N_2, CO and CO_2 molecules," J. Phys. Soc. Jpn. **53**, 2491 (1984).

[27]M. Kimura, O. Sueoka, A. Hamada, M. Takekawa, Y. Itikawa, H. Tanaka, and L. Boesten, "Remarks on total and elastic cross sections for electron and positron scattering from CO_2," J. Chem. Phys. **107**, 6616–6620 (1997).

[28]C. Szmytkowski, A. Zecca, G. Karwasz, S. Oss, K. Maciag, B. Marinkovic, R. S. Brusa, and R. Grisenti, "Absolute total cross sections for electron-CO_2 scattering at energies from 0.5 to 3000 eV," J. Phys. B: At. Mol. Phys. **20**, 5817 (1987).

[29]G. García and F. Manero, "Total cross sections for electron scattering by CO_2 molecules in the energy range 400–5000 eV," Phys. Rev. A **53**, 250–254 (1996).

[30]D. Field, N. C. Jones, S. L. Lunt, and J.-P. Ziesel, "Experimental evidence for a virtual state in a cold collision: Electrons and carbon dioxide," Phys. Rev. A **64**, 022708 (2001).

[31]J. Ferch, C. Masche, and W. Raith, "Total cross section measurement for e-CO_2 scattering down to 0.07 eV," J. Phys. B: At. Mol. Phys. **14**, L97 (1981).

[32]S. J. Buckman, M. T. Elford, and D. S. Newman, "Electron scattering from vibrationally excited CO_2," J. Phys. B: At. Mol. Phys. **20**, 5175 (1987).

[33]A. I. Lozano, A. García-Abenza, F. Blanco Ramos, M. Hasan, D. S. Slaughter, T. Weber, R. P. McEachran, R. D. White, M. J. Brunger, P. Limão-Vieira, and G. García Gómez-Tejedor, "Electron and positron scattering cross sections from CO_2: A comparative study over a broad energy range (0.1–5000 eV)," J. Phys. Chem. A **126**, 6032–6046 (2022).

[34]A. I. Lozano, J. C. Oller, K. Krupa, F. Ferreira da Silva, P. Limão-Vieira, F. Blanco, A. Muñoz, R. Colmenares, and G. García, "Magnetically confined electron beam system for high resolution electron transmission-beam experiments," Rev. Sci. Instrum. **89**, 063105 (2018).

[35]G. P. Karwasz, R. S. Brusa, and A. Zecca, "6.1 Total scattering cross sections," in *Photon and Electron Interactions with Atoms, Molecules and Ions · Interactions of Photons and Electrons with Molecules*, Landolt–Börnstein—Group I Elementary Particles, Nuclei and Atoms (Springer Materials, Springer-Verlag, Berlin, Heidelberg, 2003), Vol. 17C.

[36]E. Brüche, "Wirkungsquerschnitt und molekülbau," Ann. Phys. **388**, 1065–1128 (1927).

[37]C. Ramsauer, "Über den Wirkungsquerschnitt der Kohlensäuremoleküle gegenüber langsamen Elektronen," Ann. Phys. **388**, 1129–1135 (1927).

[38]C. Ramsauer and R. Kollath, "Über den Wirkungsquerschnitt der Nichtedelgasmoleküle gegenüber Elektronen unterhalb 1 Volt," Ann. Phys. **396**, 91–108 (1930).

[39]M. Kitajima, A. Kondo, N. Kobayashi, T. Ejiri, T. Okumura, K. Shigemura, K. Hosaka, T. Odagiri, and M. Hoshino, "High-resolution and high-precision measurements of total cross section for electron scattering from CO_2," Eur. Phys. J. D **77**, 198 (2023).

[40]G. García, C. Aragón, and J. Campos, "Total cross sections for electron scattering from CO in the energy range 380–5200 eV," Phys. Rev. A **42**, 4400–4402 (1990).

[41]I. Kanik, J. C. Nickel, and S. Trajmar, "Total electron scattering cross section measurements for Kr, O_2 and CO," J. Phys. B: At., Mol. Opt. Phys. **25**, 2189 (1992).

[42]G. Karwasz, R. S. Brusa, A. Gasparoli, and A. Zecca, "Total cross-section measurements for e^--CO scattering: 80–4000 eV," Chem. Phys. Lett. **211**, 529–533 (1993).

[43]S. L. Xing, Q. C. Shi, X. J. Chen, K. Z. Xu, B. X. Yang, S. L. Wu, and R. F. Feng, "Absolute total-cross-section measurements for intermediate-energy electron scattering on C_2H_2 and CO," Phys. Rev. A **51**, 414–417 (1995).

[44]J. Ferch, C. Masche, W. Raith, and L. Wiemann, "Electron scattering from vibrationally excited CO_2 in the energy range of the $^2\Pi_u$ shape resonance," Phys. Rev. A **40**, 5407–5410 (1989).

Published by AIP Publishing on behalf of the National Institute of Standards and Technology.

[45]M. Allan, "Excitation of vibrational levels up to $v = 17$ in N_2 by electron impact in the 0–5 eV region," J. Phys. B: At. Mol. Phys. **18**, 4511 (1985).
[46]W. M. Johnstone, M. J. Brunger, and W. R. Newell, "Differential electron scattering from the (010) excited vibrational mode of CO_2," J. Phys. B: At., Mol. Opt. Phys. **32**, 5779 (1999).
[47]M. A. Morrison, "Interpretation of the near-threshold behavior of cross sections for e-CO_2 scattering," Phys. Rev. A **25**, 1445–1449 (1982).
[48]H. Estrada and W. Domcke, "On the virtual-state effect in low-energy electron-CO_2 scattering," J. Phys. B: At. Mol. Phys. **18**, 4469 (1985).
[49]L. A. Morgan, "Virtual states and resonances in electron scattering by CO_2," Phys. Rev. Lett. **80**, 1873–1875 (1998).
[50]M. Allan, "Vibrational structures in electron–CO_2 scattering below the $^2\Pi_u$ shape resonance," J. Phys. B: At., Mol. Opt. Phys. **35**, L387 (2002).
[51]Z. Idziaszek, G. P. Karwasz, and R. S. Brusa, "Modified effective range analysis of low energy electron and positron scattering on CO_2," J. Phys.: Conf. Ser. **115**, 012002 (2008).
[52]K. Fedus and G. Karwasz, "Virtual states in electron-molecule scattering via modified effective-range theory," Phys. Rev. A **109**, 022801 (2024).
[53]T. W. Shyn, W. E. Sharp, and G. R. Carignan, "Angular distribution of electrons elastically scattered from CO_2," Phys. Rev. A **17**, 1855–1861 (1978).
[54]D. F. Register, H. Nishimura, and S. Trajmar, "Elastic scattering and vibrational excitation of CO_2 by 4, 10, 20 and 50 eV electrons," J. Phys. B: At. Mol. Phys. **13**, 1651–1662 (1980).
[55]K. H. Kochem, W. Sohn, N. Hebel, K. Jung, and H. Ehrhardt, "Elastic electron scattering and vibrational excitation of CO_2 in the threshold energy region," J. Phys. B: At. Mol. Phys. **18**, 4455–4467 (1985).
[56]I. Kanik, D. C. McCollum, and J. C. Nickel, "Absolute elastic differential scattering cross sections for electron impact on carbon dioxide in the intermediate energy region," J. Phys. B: At., Mol. Opt. Phys. **22**, 1225 (1989).
[57]H. Tanaka, T. Ishikawa, T. Masai, T. Sagara, L. Boesten, M. Takekawa, Y. Itikawa, and M. Kimura, "Elastic collisions of low- to intermediate-energy electrons from carbon dioxide: Experimental and theoretical differential cross sections," Phys. Rev. A **57**, 1798–1808 (1998).
[58]J. C. Gibson, M. A. Green, K. W. Trantham, S. J. Buckman, P. J. O. Teubner, and M. J. Brunger, "Elastic electron scattering from CO_2," J. Phys. B: At., Mol. Opt. Phys. **32**, 213 (1999).
[59]I. Iga, M. G. P. Homem, K. T. Mazon, and M.-T. Lee, "Elastic and total cross sections for electron-carbon dioxide collisions in the intermediate energy range," J. Phys. B: At., Mol. Opt. Phys. **32**, 4373 (1999).
[60]M. Takekawa and Y. Itikawa, "Elastic scattering of electrons from carbon dioxide," J. Phys. B: At., Mol. Opt. Phys. **29**, 4227 (1996).
[61]T. N. Rescigno, D. A. Byrum, W. A. Isaacs, and C. W. McCurdy, "Theoretical studies of low-energy electron-CO_2 scattering: Total, elastic, and differential cross sections," Phys. Rev. A **60**, 2186–2193 (1999).
[62]F. A. Gianturco and T. Stoecklin, "Low-energy electron scattering from CO_2 molecules: Elastic channel calculations revisited," J. Phys. B: At., Mol. Opt. Phys. **34**, 1695 (2001).
[63]S. J. Buckman, M. Brunger, and M. T. Elford, "6.2 Integral elastic cross sections," in *Photon and Electron Interactions with Atoms, Molecules and Ions · Interactions of Photons and Electrons with Molecules*, Landolt–Börnstein—Group I Elementary Particles, Nuclei and Atoms (Springer Materials, Berlin Heidelberg New York, 2003), Vol. 17C.
[64]I. Iga, J. C. Nogueira, and M.-T. Lee, "Elastic scattering of electrons from CO_2 in the intermediate energy range," J. Phys. B: At. Mol. Phys. **17**, L185–L189 (1984).
[65]R. D. Hake and A. V. Phelps, "Momentum-transfer and inelastic-collision cross sections for electrons in O_2, CO, and CO_2," Phys. Rev. **158**, 70–84 (1967).
[66]J. J. Lowke, A. V. Phelps, and B. W. Irwin, "Predicted electron transport coefficients and operating characteristics of CO_2–N_2–He laser mixtures," J. Appl. Phys. **44**, 4664–4671 (1973).
[67]M. A. Morrison, N. F. Lane, and L. A. Collins, "Low-energy electron-molecule scattering: Application of coupled-channel theory to e-CO_2 collisions," Phys. Rev. A **15**, 2186–2201 (1977).
[68]M. T. Elford, S. J. Buckman, and M. Brunger, "6.3 Elastic momentum transfer cross sections," in *Photon and Electron Interactions with Atoms, Molecules and Ions · Interactions of Photons and Electrons with Molecules*, Landolt–Börnstein—Group I Elementary Particles, Nuclei and Atoms (Springer Materials, Berlin Heidelberg New York, 2003), Vol. 17C.
[69]M. A. Morrison and N. F. Lane, "Theoretical calculation of cross sections for rotational excitation in e-CO_2 scattering," Phys. Rev. A **16**, 975 (1977).
[70]D. Thirumalai, K. Onda, and D. G. Truhlar, "Electron scattering by CO_2: Elastic scattering, rotational excitation, and excitation of the asymmetric stretch at 10 eV impact energy," J. Chem. Phys. **74**, 6792–6805 (1981).
[71]F. A. Gianturco and T. Stoecklin, "Calculation of rotationally inelastic processes in electron collisions with CO_2 smolecules," Phys. Rev. A **55**, 1937 (1997).
[72]W. Vanroose, C. W. McCurdy, and T. N. Rescigno, "Interpretation of low-energy electron-CO_2 scattering," Phys. Rev. A **66**, 032720 (2002).
[73]T. Antoni, K. Jung, H. Ehrhardt, and E. Chang, "Rotational branch analysis of the excitation of the fundamental vibrational modes of CO_2 by slow electron collisions," J. Phys. B: At. Mol. Phys. **19**, 1377 (1986).
[74]M. Kitajima, S. Watanabe, H. Tanaka, M. Takekawa, M. Kimura, and Y. Itikawa, "Differential cross sections for vibrational excitation of CO_2 by 1.5–30 eV electrons," J. Phys. B: At., Mol. Opt. Phys. **34**, 1929 (2001).
[75]G. B. Poparic, M. M. Ristic, and D. S. Belic, "Electron energy transfer rate coefficients of carbon dioxide," J. Phys. Chem. A **114**, 1610–1615 (2010).
[76]C. Szmytkowski, M. Zubek, and J. Drewko, "Calculation of cross sections for vibrational excitation and de-excitation of CO_2 by electronic collisions," J. Phys. B: At. Mol. Phys. **11**, L371 (1978).
[77]A. Kazansky and L. Y. Sergeeva, "On the local theory of resonant inelastic collisions of slow electrons with carbon dioxide," J. Phys. B: At., Mol. Opt. Phys. **27**, 3217 (1994).
[78]A. Kazanskii, "Calculation of cross sections for inelastic collisions of slow electrons with triatomic molecules: A three-mode model of collisions of electrons with carbon dioxide," Opt. Spectrosc. **87**, 840–846 (1999).
[79]T. N. Rescigno, W. A. Isaacs, A. E. Orel, H.-D. Meyer, and C. W. McCurdy, "Theoretical study of resonant vibrational excitation of CO_2 by electron impact," Phys. Rev. A **65**, 032716 (2002).
[80]C. W. McCurdy, W. A. Isaacs, H.-D. Meyer, and T. N. Rescigno, "Resonant vibrational excitation of CO_2 by electron impact: Nuclear dynamics on the coupled components of the $^2\Pi_u$ resonance," Phys. Rev. A **67**, 042708 (2003).
[81]L. Pietanza, G. Colonna, V. Laporta, R. Celiberto, G. D'Ammando, A. Laricchiuta, and M. Capitelli, "Influence of electron molecule resonant vibrational collisions over the symmetric mode and direct excitation-dissociation cross sections of CO_2 on the electron energy distribution function and dissociation mechanisms in cold pure CO_2 plasmas," J. Phys. Chem. A **120**, 2614–2628 (2016).
[82]V. Laporta, J. Tennyson, and R. Celiberto, "Calculated low-energy electron-impact vibrational excitation cross sections for CO_2 molecule," Plasma Sources Sci. Technol. **25**, 06LT02 (2016).
[83]M. Allan, "Selectivity in the excitation of fermi-coupled vibrations in CO_2 by impact of slow electrons," Phys. Rev. Lett. **87**, 033201 (2001).
[84]H. Kawahara, H. Kato, M. Hoshino, H. Tanaka, L. Campbell, and M. J. Brunger, "Integral cross sections for electron impact excitation of the $^1\Sigma_u^+$ and $^1\Pi_u$ electronic states in CO_2," J. Phys. B: At., Mol. Opt. Phys. **41**, 085203 (2008).
[85]M. A. Green, P. J. O. Teubner, L. Campbell, M. Brunger, M. Hoshino, T. Ishikawa, M. Kitajima, H. Tanaka, Y. Itikawa, M. Kimura, and R. J. Buenker, "Absolute differential cross sections for electron impact excitation of the 10.8–11.5 eV energy-loss states of CO_2," J. Phys. B: At., Mol. Opt. Phys. **35**, 567 (2002).
[86]K. N. Klump and E. N. Lassettre, "Generalized oscillator strengths for two transitions in CO_2 at incident electron energies of 300, 400 and 500 eV," J. Electron Spectrosc. Relat. Phenom. **14**, 215–230 (1978).
[87]S.-X. Wang and L.-F. Zhu, "Integral cross sections for electron impact excitations of argon and carbon dioxide," Chin. Phys. B **31**, 083401 (2022).
[88]C. W. McCurdy, Jr. and V. McKoy, "Equations of motion method: Inelastic electron scattering for helium and CO_2 in the Born approximation," J. Chem. Phys. **61**, 2820–2826 (1974).
[89]L. Mu-Tao and V. McKoy, "Cross sections for electron impact excitation of the low-lying electron states of CO_2," J. Phys. B: At. Mol. Phys. **16**, 657 (1983).
[90]C.-H. Lee, C. Winstead, and V. McKoy, "Collisions of low-energy electrons with CO_2," J. Chem. Phys. **111**, 5056–5066 (1999).
[91]J. M. Carr, P. Galiatsatos, J. D. Gorfinkiel, A. G. Harvey, M. Lysaght, D. Madden, Z. Mašín, M. Plummer, J. Tennyson, and H. N. Varambhia,

"UKRmol: A low-energy electron-and positron-molecule scattering suite," Eur. Phys. J. D **66**, 58 (2012).
[92]J. Tennyson, D. B. Brown, J. J. Munro, I. Rozum, H. N. Varambhia, and N. Vinci, "Quantemol-N: An expert system for performing electron molecule collision calculations using the R-matrix method," J. Phys.: Conf. Ser. **86**, 012001 (2007).
[93]H.-J. Werner, P. J. Knowles, G. Knizia, F. R. Manby, and M. Schütz, "Molpro: A general-purpose quantum chemistry program package," Wiley Interdiscip. Rev.: Comput. Mol. Sci. **2**, 242–253 (2012).
[94]C. Cosby and H. Helm, "Dissociation rates of diatomic molecules," report No. AD-A266 464 WL-TR-93-2004, Wright-Patterson Airforce Base, Dayton, OH, 1992.
[95]A. Bogaerts, W. Wang, A. Berthelot, and V. Guerra, "Modeling plasma-based CO_2 conversion: Crucial role of the dissociation cross section," Plasma Sources Sci. Technol. **25**, 055016 (2016).
[96]P. C. Cosby, "Electron-impact dissociation of nitrogen," J. Chem. Phys. **98**, 9544 (1993).
[97]L. R. LeClair and J. W. McConkey, "On $O(^1S)$ and $CO(a\ ^3\Pi)$ production from electron impact dissociation of CO_2," J. Phys. B: At., Mol. Opt. Phys. **27**, 4039 (1994).
[98]H. C. Straub, B. G. Lindsay, K. A. Smith, and R. F. Stebbings, "Absolute partial cross sections for electron-impact ionization of CO_2 from threshold to 1000 eV," J. Chem. Phys. **105**, 4015–4022 (1996).
[99]C. Montesano, T. P. Salden, L. M. Martini, G. Dilecce, and P. Tosi, "CO_2 reduction by nanosecond-plasma discharges: Revealing the dissociation's time scale and the importance of pulse sequence," J. Phys. Chem. C **127**, 10045–10050 (2023).
[100]R. K. Asundi, J. D. Craggs, and M. V. Kurepa, "Electron attachment and ionization in oxygen, carbon monoxide and carbon dioxide," Proc. Phys. Soc. **82**, 967 (1963).
[101]D. Rapp and P. Englander-Golden, "Total cross sections for ionization and attachment in gases by electron impact. I. Positive ionization," J. Chem. Phys. **43**, 1464–1479 (1965).
[102]J. E. Hudson, C. Vallance, and P. W. Harland, "Absolute electron impact ionization cross-sections for CO, CO_2, OCS and CS_2," J. Phys. B: At., Mol. Opt. Phys. **37**, 445 (2003).
[103]B. Adamczyk, A. J. H. Boerboom, and M. Łukasiewicz, "Partial ionization cross sections of carbon dioxide by electrons (25–600 eV)," Int. J. Mass Spectrom. Ion Phys. **9**, 407–412 (1972).
[104]B. Adamczyk, K. Bederski, and L. Wójcik, "Mass spectrometric investigation of dissociative ionization of toxic gases by electrons at 20–1000 eV," Biol. Mass Spectrom. **16**, 415–417 (1988).
[105]A. Crowe and J. W. McConkey, "Dissociative ionization by electron impact. III. O^+, CO^+ and C^+ from CO_2," J. Phys. B: At. Mol. Phys. **7**, 349 (1974).
[106]T. D. Märk and E. Hille, "Cross section for single and double ionization of carbon dioxide by electron impact from threshold up to 180 eV," J. Chem. Phys. **69**, 2492–2496 (1978).
[107]C. Tian and C. R. Vidal, "Electron impact dissociative ionization of CO_2: Measurements with a focusing time-of-flight mass spectrometer," J. Chem. Phys. **108**, 927–936 (1998).
[108]R. S. Freund, R. C. Wetzel, and R. J. Shul, "Measurements of electron-impact-ionization cross sections of N_2, CO, CO_2, CS, S_2, CS_2, and metastable N_2," Phys. Rev. A **41**, 5861–5868 (1990).
[109]O. J. Orient and S. K. Srivastava, "Production of O^- from CO_2 by dissociative electron attachment," Chem. Phys. Lett. **96**, 681–684 (1983).
[110]S. J. King and S. D. Price, "Electron ionization of CO_2," Int. J. Mass Spectrom. **272**, 154–164 (2008).
[111]B. G. Lindsay and M. A. Mangan, "Interactions of photons and electrons with molecules · 5.1 Ionization," in *Photon and Electron Interactions with Atoms, Molecules and Ions · Interactions of Photons and Electrons with Molecules*, Landolt–Börnstein—Group I Elementary Particles, Nuclei and Atoms (Springer Materials, Springer-Verlag, Berlin, Heidelberg, 2003), Vol. 17C.
[112]O. J. Orient and S. K. Strivastava, "Electron impact ionisation of H_2O, CO, CO_2 and CH_4," J. Phys. B: At. Mol. Phys. **20**, 3923 (1987).
[113]G. P. Karwasz, P. Możejko, and M.-Y. Song, "Electron-impact ionization of fluoromethanes—Review of experiments and binary-encounter models," Int. J. Mass Spectrom. **365–366**, 232–237 (2014).
[114]P. Verma and R. J. Bartlett, "Increasing the applicability of density functional theory. IV. Consequences of ionization-potential improved exchange-correlation potentials," J. Chem. Phys. **140**, 18A534 (2014).
[115]E. Krishnakumar, "A pulsed crossed beam apparatus for measurement of electron impact partial ionisation cross-sections: Results on CO_2," Int. J. Mass Spectrom. Ion Processes **97**, 283–294 (1990).
[116]J. W. McConkey, D. J. Burns, and J. M. Woolsey, "Absolute cross sections for ionization and excitation of CO_2 by electron impact," J. Phys. B: At. Mol. Phys. **1**, 71 (1968).
[117]J. M. Ajello, "Emission cross sections of CO_2 by electron impact in the interval 1260–4500 Å. II," J. Chem. Phys. **55**, 3169–3177 (1971).
[118]S. Tsurubuchi and T. Iwai, "Simultaneous ionization and excitation of CO_2 by electron-impact," J. Phys. Soc. Jpn. **37**, 1077–1081 (1974).
[119]C. Tian and C. R. Vidal, "Single to quadruple ionization of CO_2 due to electron impact," Phys. Rev. A **58**, 3783–3795 (1998).
[120]V. Sharma, B. Bapat, J. Mondal, M. Hochlaf, K. Giri, and N. N. Sathyamurthy, "Dissociative double ionization of CO_2: Dynamics, energy levels, and lifetime," J. Phys. Chem. A **111**, 10205–10211 (2007).
[121]P. Bhatt, R. Singh, N. Yadav, and R. Shanker, "Dissociative-ionization cross sections for 12-keV-electron impact on CO_2," Phys. Rev. A **84**, 042701 (2011).
[122]P. Bhatt, R. Singh, N. Yadav, and R. Shanker, "Formation, structure, and dissociation dynamics of CO_2^{q+} ($q \leq 3$) ions due to impact of 12-keV electrons," Phys. Rev. A **85**, 042707 (2012).
[123]E. Wang, X. Shan, Y. Shi, Y. Tang, and X. Chen, "Momentum imaging spectrometer for molecular fragmentation dynamics induced by pulsed electron beam," Rev. Sci. Instrum. **84**, 123110 (2013).
[124]X. Wang, Y. Zhang, D. Lu, G. C. Lu, B. Wei, B. H. Zhang, Y. J. Tang, R. Hutton, and Y. Zou, "Fragmentation CO_2^{2+} of in collisions with low-energy electrons," Phys. Rev. A **90**, 062705 (2014).
[125]D. Spence and G. J. Schulz, "Cross sections for production of O_2^- and C^- by dissociative electron attachment in CO_2: An observation of the Renner-Teller effect," J. Chem. Phys. **60**, 216–220 (1974).
[126]P. Nag and D. Nandi, "Dissociation dynamics in the dissociative electron attachment to carbon dioxide," Phys. Rev. A **91**, 052705 (2015).
[127]D. Ascenzi, C. Romanzin, A. Lopes, P. Tosi, J. Žabka, M. Polášek, C. J. Shaffer, and C. Alcaraz, "State-selected reactivity of carbon dioxide cations (CO_2^+) with methane," Front. Chem. **7**, 537 (2019).
[128]L. Gkouvelis, J.-C. Gérard, B. Ritter, B. Hubert, N. M. Schneider, and S. K. Jain, "The $O(^1S)$ 297.2-nm dayglow emission: A tracer of CO_2 density variations in the Martian lower thermosphere," J. Geophys. Res.: Planets **123**, 3119–3132 (2018).
[129]Q. Zhang, H. Gu, J. Cui, Y.-M. Cheng, Z.-G. He, J.-H. Zhong, F. He, and Y. Wei, "Atomic oxygen escape on Mars driven by electron impact excitation and ionization," Astron. J. **159**, 54 (2020).
[130]K. Seiersen, A. Al-Khalili, O. Heber, M. J. Jensen, I. B. Nielsen, H. B. Pedersen, C. P. Safvan, and L. H. Andersen, "Dissociative recombination of the cation and dication of CO_2," Phys. Rev. A **68**, 022708 (2003).
[131]A. A. Viggiano, A. Ehlerding, F. Hellberg, R. D. Thomas, V. Zhaunerchyk, W. D. Geppert, H. Montaigne, M. Larsson, M. Kaminska, and F. Österdahl, "Rate constants and branching ratios for the dissociative recombination of CO_2^+," J. Chem. Phys. **122**, 226101 (2005).
[132]C. S. Weller and M. A. Biondi, "Measurements of dissociative recombination of CO_2^+ ions with electrons," Phys. Rev. Lett. **19**, 59–61 (1967).
[133]R. A. Gutcheck and E. C. Zipf, "Excitation of the CO fourth positive system by the dissociative recombination of CO_2^+ ions," J. Geophys. Res. **78**, 5429–5436 (1973).
[134]M. Geoghegan, N. G. Adams, and D. Smith, "Determination of the electron-ion dissociative recombination coefficients for several molecular ions at 300 K," J. Phys. B: At., Mol. Opt. Phys. **24**, 2589 (1991).
[135]T. Gougousi, M. F. Golde, and R. Johnsen, "Electron-ion recombination rate coefficient measurements in a flowing afterglow plasma," Chem. Phys. Lett. **265**, 399–403 (1997).

[136]A. Müller, E. Salzborn, R. Frodl, R. Becker, and H. Klein, "Ionisation of CO_2^+ ions by electron impact," J. Phys. B: At. Mol. Phys. **13**, L221 (1980).
[137]E. M. Bahati, J. J. Jureta, D. S. Belic, S. Rachafi, and P. Defrance, "Electron impact ionization and dissociation of CO_2^+ to C^+ and O^+," J. Phys. B: At., Mol. Opt. Phys. **34**, 1757 (2001).
[138]H. Deutsch, K. Becker, P. Defrance, U. Onthong, R. Parajuli, M. Probst, S. Matt, and T. D. Märk, "Calculated absolute cross section for the electron-impact ionization of CO_2^+ and N_2^+," J. Phys. B: At. Mol. Opt. Phys. **35**, L65 (2002).
[139]Y. K. Kim, K. K. Irikura, and M. A. Ali, "Electron-impact total ionization cross sections of molecular ions," J. Res. Natl. Inst. Stand. Technol. **105**, 285 (2000).